Age-related decline of stand biomass accumulation is primarily due to mortality and not to reduction in NPP associated with individual tree physiology, tree growth or stand structure in a Quercus-dominated forest

Author

Xu, Cheng-Yuan, Turnbull, Matthew H, Tissue, David T, Lewis, James D, Carson, Rob, Schuster, William SF, Whitehead, David, Walcroft, Adrian S, Li, Jinbao, Griffin, Kevin L

Published

2012

Journal Title

Journal of Ecology

DOI

10.1111/j.1365-2745.2011.01933.x

Age-related decline of stand biomass accumulation is primarily due to mortality and not to reduction in NPP associated with individual tree physiology, tree growth or stand structure in a *Quercus*-dominated forest

CHENG-YUAN XU[1,2*], MATTHEW H. TURNBULL[3], DAVID T. TISSUE[4,5], JAMES D. LEWIS[5,6], ROB CARSON[7], WILLIAM S. F. SCHUSTER[8], DAVID WHITEHEAD[9], ADRIAN S. WALCROFT[9], JINBAO LI[10], KEVIN L. GRIFFIN[10]

[1] *Department of Biological and Physical Science, University of Southern Queensland Toowoomba, QLD 4350, Australia*

[2] *CSIRO Ecosystem Sciences, EcoSciences Precinct, Boggo Road, Dutton Park, QLD 4102, Australia*

[3] *School of Biological Sciences, University of Canterbury, Private Bag 4800, Christchurch, New Zealand*

[4] *Department of Biology, Texas Tech University, Lubbock, TX 79409 USA*

[5] *Hawkesbury Institute for the Environment, University of Western Sydney, Richmond NSW 2753 Australia*

[6] *Louis Calder Center, Fordham University, 53 Whippoorwill Rd., Box 887 Armonk, NY 10504, USA*

[7] *Department of Ecology, Evolution, and Environmental Biology, Columbia University, New York, NY 10025, USA*

[8] *Block Rock Forest Consortium, 129 Continental Road, Cornwall, New York 12518, USA*

[9] *Landcare Research, PO Box 40, Lincoln 7640, New Zealand*

[10] *Lamont-Doherty Earth Observatory, Columbia University, Palisades NY 10964, USA*

[*] **Correspondence author:** Department of Biological and Physical Science, University of Southern Queensland, West Street, Toowoomba, QLD 4350, Australia; Email: chengyuan-stephen.xu@usq.edu.au; Fax: 61-7-46352175; Phone: 61-7-46312214

The type of article: Standard paper

Running title: Age-related decline in a *Quercus* forest

Summary

1. Age-related reductions in stand biomass accumulation are frequently observed in old-growth forests. The phenomenon may be caused by reduced production, increased mortality, or both. The relative importance of production and mortality is not well studied, so the mechanisms controlling age-related decline of stand biomass accumulation remain unclear.

2. In this study, conducted in a *Quercus*-dominated deciduous forest in the Northeastern USA, we examined whether age-related decline in stand above-ground biomass accumulation could be explained by reduction of above-ground NPP (growth of surviving trees) that may be associated with (i) physiological constraints within individual trees or (ii) changes in stand structure, or by (iii) age-related, increasing tree mortality in stands up to 135 years old. Few previous studies have tested these hypotheses simultaneously within the same forest.

3. We did not find evidence for a reduction in individual tree growth associated with age-related physiological constraints, in terms of foliar carbon assimilation capacity, photosynthesis/ respiration balance, nitrogen availability or hydraulic constraints on carbon gain. Over the period of 1937 to 2006, we did not observe alterations in stand structure and the above-ground NPP of the *Quercus* forest was generally stable.

4. However, we did find that the primary mechanism driving age-related decline of stand above-ground biomass accumulation was biomass loss due to the death of large, dominant trees. Our results indicate that shifts in mortality from the loss of small trees to the loss of large trees, rather than changes in above-ground NPP, drives age-related decline in stand above-ground biomass accumulation in this forest.

5. Synthesis: We found that within the range of stand development stages analyzed, the age-related decline of stand above-ground biomass accumulation in a *Quercus*-dominated forest was primarily due to mortality of large, dominant trees and not due to changes in above-ground NPP associated with tree physiology, individual tree growth, or stand structure. This result indicates that tree demography and the influence of climate change on disturbances may need to be integrated into models to predict the change of above-ground carbon stock of some old-growth forests.

Key-words: carbon sequestration, disturbance, ecophysiology, growth dominance, hydraulic limitation, net primary productivity, nitrogen, photosynthesis, respiration, temperate deciduous forest

Introduction

Forest woody biomass is an important global carbon stock, so it is critical to understand the dynamics of biomass accumulation of forest stands (Cooper 1983). It is generally accepted that the rate of stand biomass accumulation peaks in the early stage of development, usually at the time of canopy closure or peak stand leaf area, and declines thereafter. Such age-related decline in stand biomass accumulation has been widely observed in various empirical studies (Turner & Long 1975; Binkley & Greene 1983; Grier *et al.* 1989; Acker *et al.* 2002; Taylor & MacLean 2005; McMahon, Parker & Miller 2010), potentially reducing the capacity for forests to become sinks for carbon (Hurtt *et al.* 2002).

Stand biomass accumulation is the net result of production and mortality. Therefore, age-related decline of stand biomass accumulation could be attributable to declined production, increased mortality, or both. Age-related decline in net primary production (NPP) has been widely observed and studied extensively (see review, Gower, McMurtrie & Murty 1996; Ryan, Binkley & Fownes 1997) and is shown to be primarily responsible for a decline in the rate of stand biomass accumulation in some cases. For example, in Douglas-fir forests of the Pacific Northwest U. S., stand biomass accumulation was closely associated to NPP, particularly for early stages of stand development (Grier *et al.* 1989). Alternatively, long-term studies in several old-growth stands have showed that mortality is roughly equal to or higher than production of surviving trees, and thus stand biomass accumulation is close to zero or negative (Grier & Logan 1977; Binkley & Greene 1983; DeBell & Franklin 1987). Given the fact that the production of surviving trees of old-growth stands was in general significantly lower than that of younger stands in these early studies, Ryan, Binkley & Fownes (1997) concluded that "low net growth rate in old-growth stands apparently results from poor growth (i.e. declining growth of surviving trees), not high mortality". However, more recent

empirical studies have not supported this conclusion. For instance, in some coniferous forests, it was found that mortality could be an equally important or a primary factor that contributed to reduced biomass accumulation in old-growth stands (Acker *et al.* 2002; Taylor & MacLean 2005). In summary, the relative importance of production and mortality in shaping the age-related decline of stand biomass accumulation is not well understood, and the mechanisms responsible for age-related decline in forest biomass accumulation remains uncertain.

The age-related decline of forest stand biomass accumulation is commonly interpreted as the consequence of a large decrease in productivity as forest aging, but the mechanism causing age-related decline of NPP remains unclear. Numerous hypotheses have been developed to explain the phenomenon as a function of age- or size-dependent physiological constraints leading to reductions in growth of individual trees (see review, Gower, McMurtrie & Murty 1996; Ryan, Binkley & Fownes 1997; Smith & Long 2001; Weiner & Thomas 2001), including (i) photosynthesis–respiration imbalance, (ii) increased nutrient limitation, (iii) increased hydraulic resistance, and (iv) reduced allocation to stem production. In addition, Ryan, Binkley & Fownes (1997) and Bond (2000) suggest that genetic changes associated with older meristems may constrain growth of trees as they age, but this has not been experimentally confirmed. Alternatively, age-related decline of forest NPP has also been described as an emergent property of stand dynamics linked to structural change within the forest. Binkley (2004) proposed that near canopy closure, the increasing dominance of large trees would lead to declining resource use efficiency of non-dominant trees as the result of intensified competition, and hence reduced stand growth; during further stand development, stand decline was attributed to the inability of larger, older trees to maintain growth despite their dominance in resource use. Similar hypotheses were also suggested by Smith & Long (2001). Testing these hypotheses is problematic because sufficiently long-term growth data from old forests are rare. Subsequently, most studies addressing stand-structure hypotheses

can only address a few key expectations (Binkley *et al.* 2002; Binkley 2004; Fernandez & Gyenge 2009).

Mortality of older trees is a stand-level phenomenon that may reduce forest stand biomass accumulation through two pathways. First, intuitively, biomass loss due to mortality reduces living biomass and may be the primary factor to affect forest biomass accumulation. This mechanism has been supported by two recent empirical studies in conifer forests (Acker *et al.* 2002; Taylor & MacLean 2005). Second, mortality could temporarily remove leaf area and thus decrease NPP. Some studies suggest that mortality does not occur frequently enough to significantly reduce productivity in older forests (Ryan, Binkley & Fownes 1997), but a more recent model simulation indicates that biomass loss due to mortality of larger, older trees which cannot be compensated for through higher production by smaller trees, may dominate the later stage of forest decline (Berger, Hildenbrandt & Grimm 2004). Overall, more empirical studies are needed to examine the role of mortality in shaping stand biomass accumulation over the age.

Although these major hypotheses associated with age-related decline of stand biomass accumulation have been individually tested for decades in numerous studies, results are not consistent, thereby generating debate among ecologists. One particular knowledge gap is that few studies have examined multiple mechanisms simultaneously within the same forest. In this study, conducted in a *Quercus*-dominated deciduous forest in the Northeastern USA, we examined whether age-related decline of stand above-ground biomass accumulation could be explained by reduction in above-ground NPP that may be associated with (i) physiological constraints in individual trees (including photosynthesis-respiration imbalance, nutrient limitation, and hydraulic constraint) or (ii) changes in stand structure and canopy dominance; or by (iii) increasing biomass loss due to age-related tree death, recognizing that these

mechanisms were not mutually exclusive. Ultimately, we need to understand the mechanisms controlling age-related decline of forest stand biomass accumulation to accurately predict the long-term capacity of forests to sequester carbon in living woody biomass.

Material and methods

Study site

Black Rock Forest (BRF) is a 1500 ha preserve in the Hudson Highlands region of New York (41˚24'N, 74˚01'W). It has been managed as a preserve without significant disturbance since 1928. The forest is *Quercus*-dominated (see Appendix *Method*), typical of secondary growth forests that characterize the Northeastern United States (Schuster *et al.* 2008). For the most dominant species *Q. rubra*, the oldest trees that have been dated by tree-ring analysis are about 150 years old (N. Pederson, personal communication). Details of the BRF are reported in (Schuster *et al.* 2008). This research was conducted on four *Q. rubra* dominated neighbouring stands that formed a chronosequence (35-, 70-, 90-, and 135-year plots) and eight long-term monitored plots that aged between 98–123 years in 2006 and were monitored since 1937 (Fig. 1a, Appendix Table S1). Although the age-span in this study does not cover the entire life span of *Quercus* spp., it is representative of the current status of regenerating *Quercus* deciduous forests in the Northeastern U. S. (see Appendix Fig. S1). Tree species composition and estimated living above-ground biomass (AGB) of studied plots is shown in Fig. 1 (b, c).

Study design

We first confirmed the age-related decline of stand AGB accumulation in the BRF by comparing AGB of chronosequence plots and traced the last 70 years of AGB development on long-term plots. Then, we examined whether the observed age-related decline could be explained by (H1) changes in tree physiology related to photosynthesis-respiration balance, nutrient limitation, and/or hydraulic constraints; (H2) changing stand structure as reflected by growth dominance; or (H3) age-related change in mortality. H1 and H2 mainly affect stand

AGB accumulation through reducing NPP while H3 directly cause biomass loss and may reduce NPP.

H1 was tested based upon six sub-hypotheses: H1-1: The capacity of foliar carbon fixation decreases with tree age; H1-2: The ratio of photosynthesis to respiration (foliar A/R and whole tree foliar photosynthesis/ woody respiration) decreases with tree age; H1-3: Foliar nitrogen and protein decrease, while carbon to nitrogen ratio (C/N) increases with tree age; H1-4: Hydraulic limitations to carbon gain increase with tree age; H1-5: The AGB growth of individual trees and the growth efficiency (i.e. AGB growth relative to the leaf area sustained) decreases with tree age, given that the physiological constraints examined in H1-1 to H1-4 would finally limit the growth of individual trees (Weiner & Thomas 2001); and H1-6: The canopy annual net foliar exchange decreases with stand age. These sub-hypotheses were tested by measuring tree physiological characteristics of the dominant tree species, *Q. rubra*, within the stand chronosequence plots. H1-1 was tested by comparing leaf gas exchange parameters and Rubisco activity. To test H1-2, foliar A/R was calculated and the ratio of whole tree foliar photosynthesis to woody respiration was estimated by the formula (A × total leaf area of the tree) / (stem CO_2 efflux rate × trunk area of the tree) with the area-based stem CO_2 efflux data of 35-, 90- and 135-year plots from (Bowman 2005). H1-3 was examined by measuring foliar nitrogen, carbon and protein components. Tree height, leaf carbon stable isotope ratio ($\delta^{13}C$) and tree Huber value (conducting xylem area: supported leaf area) were combined to assess H1-4. H1-5 was assessed by estimating AGB growth rate utilizing allometric relationships and tree-ring width records. H1-6 was tested by modelling canopy net carbon exchange of studied plots. We did not address allocation hypotheses because this study focused on AGB in the BRF.

H2 was tested with survey data of long-term plots and compared to the prediction (Binkley 2004) that "the decline in stand-level growth near canopy closure is driven by increasing dominance of larger trees, leading to declining efficiency of resource use of smaller trees; with further stand development,…old trees enter a phase where their growth no longer keeps pace with their increasing dominance of site resources." A full test of this hypothesis was difficult due to the lack of historical data on resource use efficiency, so we only tested the key expectation that tree growth dominance would initially increase and then subsequently decrease throughout the survey period (1937–2006).

H3 was tested based upon two sub-hypothesis: H3-1: age-related decline of stand AGB accumulation is mainly caused by increasing mortality biomass loss; H3-2: age-related decline of stand AGB accumulation is mainly caused by increasing mortality-led NPP loss. H3 was addressed by analyzing the record of AGB accumulation, above-ground NPP and mortality in long-term plots during 1937–2006. If H3-1 was supported, we predicted that mortality biomass loss would increase with stand development while above-ground NPP (i.e. growth of the trees that survived the measurement period, Binkley & Arthur 1993) would be stable or increase through time. If H3-2 was supported, we predicted that above-ground NPP would decline over time and be correlated with mortality.

Above-ground biomass

The AGB of 15 of the most abundant species recorded in BRF surveys was estimated from the diameter at breast height (1.3m *D*) using allometric regression equations ($AGB=aD^b$, see Appendix Table S2 for parameters a and b, Brenneman *et al.* 1978). Allometric studies of *Q. rubra* and *Q. prinus* in the BRF indicated that these equations were the most accurate among the available ones and were developed in locations with similar site conditions and species

composition to the BRF (Schuster *et al.* 2008). For the other 11 less common species, we used the general New-York-State-derived hardwood equation of (Monteith 1979) (see Appendix Table S2). Living materials in tree stumps, roots and understorey vegetation were omitted from these formulae. The individual AGB estimates were summed to estimate AGB for each plot.

Leaf physiology and chemistry

In June 2003, 12–23 *Q. rubra* trees were selected for each chronosequence plot. Physiological measurements were conducted on one sunlit upper canopy leaf for each tree. A steady-state response of photosynthesis (A) to internal leaf CO_2 partial pressure (A-C_i Curve) and a respiratory temperature response curve were generated on the same leaf. The photosynthesis (A, 300 μmol mol^{-1} C_i and saturating light) and respiration (R) rates were reported in area-, mass- and nitrogen- based units. The A-C_i curves were fitted to a mechanistic model (Farquhar, Caemmerer & Berry 1980), and respiration–temperature curves were fitted to a modified Arrhenius equation. Parameters including the maximum carboxylation rate of Rubisco (V_{cmax}), RuBP regeneration capacity mediated by maximum electron transport rate (J_{max}), respiration rate at a base temperature (R_0), temperature response coefficient (E_0), and the commonly used Q_{10}, were calculated. The leaf material was then used to determine specific leaf area (SLA), protein content, Rubisco activity, leaf nitrogen (on area and mass basis, N_{area} and N_{mass}), C/N and $\delta^{13}C$. The photosynthetic nitrogen use efficiency (PNUE) at A was calculated as the photosynthetic rate per gram of leaf nitrogen. The details of gas exchange measurements, curve fitting and leaf analysis are described in Appendix *Methods*.

The same measurements were repeated in mid-September and late-October on a subset of six randomly selected trees in the 35-, 90-, and 135-year plots.

Tree characteristics and tree-ring growth

For each tree, we measured *D*, tree height, and sapwood area. Foliar biomass was calculated using allometric equations (after Hocker & Earley 1983; see Appendix Table S2). Total tree leaf area was estimated for each tree using foliar biomass and SLA. Huber value was calculated as sapwood cross-sectional area per unit leaf area (Tyree & Ewers 1991). Details of these measurements are described in Appendix *Methods*.

A tree core taken low on the trunk was used to age the tree and determine tree growth rate through time. Tree-ring growth was determined for each core and average AGB growth during 1998–2002 was calculated for each tree using the incremental ring-width and the allometric relationship. The AGB growth per unit leaf area was also calculated to compare the growth efficiency between age classes. Age determination was achieved using the cross-dating method and the long-term AGB accumulation trajectory was determined using the cross-dated ring-width and the allometric relationship for 1877–2002. We also calculated the historical AGB growth rate and the relative growth rate (RGR) of AGB, as $(\ln Mass_n - \ln Mass_{n-1})/1$ (year), where $Mass_n$ and $Mass_{n-1}$ respectively represented tree ABG of the current and the previous year.

Canopy net carbon exchange

The one-dimensional, multilayer model NEEMo was used to assess the age effect on annual photosynthesis and respiration of the canopy for each stand in the chronosequence (see Appendix *Methods* and Appendix Table S4 for a brief description; Whitehead *et al.* 2004a;

Whitehead *et al.* 2004b). Stand leaf area index (L) was measured using litter traps and hemispherical photographs (see Appendix *Methods*). The litter trap results were used to calculate the relative contribution of each species (f) while the hemispherical photograph results, which allow adjustment for seasonal variation of L, were used to model canopy carbon exchange.

Daily weather data for 2003 (recorded by the BRF environmental monitoring network) was used in the model to estimate annual gross primary productivity (A_G), annual night-time foliar respiration (R_f), and annual net foliar exchange (A_N=A_G-R_f). These values were multiplied by the canopy fraction of *Quercus spp.* (f_Q), assuming that the gas exchange properties of other *Quercus* species were the same as *Q. rubra*. The canopy quantum yield of electron transport (α_{can}), canopy absorbance of photosynthetically active radiation (Q_{can}) and annual canopy light use efficiency (ε_{can}, defined as the molar ratio of A_G to Q_{can}) were calculated. The sensitivities of the model to the photosynthetic parameters V_{cmax}, J_{max}, L, R_0 or E_0 were estimated by increasing or decreasing each of these five parameters up to 40% and re-running the model with no changes in values of other parameters.

Stand dominance

Stand growth dominance was analyzed with the growth survey data of 1189 trees within the eight long-term plots from 1937–2006, with the number of live trees surveyed for each decade (1937–1946 to 1997–2006) ranging between 450 and 817. For each decade, all trees surviving the whole period were ranked by biomass (decadal mean) from the smallest to largest, and then used to estimate the growth dominance: a cumulative curve was plotted with cumulative growth (annual) against cumulative biomass (Binkley 2004; Binkley *et al.* 2006), and a coefficient of growth dominance (CGD) was calculated (defined as the area below the

1:1 line minus the area below the growth dominance curve, as a proportion of the area beneath the 1:1 line, -1 < CGD < 1, Binkley *et al.* 2006). Overall, positive CGD indicate growth dominance, i.e. the growth of large trees is greater than their contribution to total stand mass, and *vice versa* (termed as reverse dominance).

Stand AGB accumulation, above-ground NPP and mortality loss

Stand AGB accumulation, above-ground NPP and mortality losses were estimated in the eight long-term plots mentioned above. Stand AGB accumulation was estimated as the difference of total living AGB between two observations; mortality loss was defined as the AGB loss of all trees that died during the observation interval; and above-ground NPP was the total growth of all surviving trees, including in-growth (trees growing into the smallest inventoried size class) and growth of surviving trees. These variables were estimated for each plot on a decadal basis and presented as annual averages (see Appendix *Methods*).

Mortality rate and structure

Mortality dominance was assessed for the loss of individual and AGB using a similar approach to that used to analyze growth dominance. The number of trees that died in each plot was counted for each decade, and then averaged to get an annual mean (individual ha^{-1} yr^{-1}). Annual tree deaths (of individual or AGB loss) and AGB data of all surveyed trees were then used to plot cumulative curves of mortality and to calculate a coefficient of mortality dominance for individuals (CMD-IND) and biomass (CMD-AGB), respectively, for each decade. The annual mortality (m) and an exponential mortality coefficient (λ) was calculated with the standard approach of $\lambda=\ln(N_0/N_t)/t$ and $m=1-e^{-\lambda}$ (Sheil, Burslem & Alder 1995), where N_0 is the number of living trees observed at the beginning of a decade; N_t is the

number of trees within the same cohort that survived until the end of the decade; t=10 (years) is the observation interval.

Data analysis

A one-way analysis of variance (ANOVA) was used to test the age effect for all variables related to leaf physiology and tree characteristics of the chronosequence. The interactive effects of season and age on leaf physiology were tested using a repeated measurement ANOVA. Significance threshold was set at P=0.05 and data were log or square root transformed to fulfil the assumptions of normality and homoscedasticity. Where significant age effect was detected, Fisher's LSD was used for multiple comparisons among age-classes. The long-term trend of tree-ring growth was fitted using linear regression.

The effect of age on stand AGB accumulation, mortality loss and above-ground NPP was analyzed with ANCOVA, with plot as a main factor to account for the effect of initial stand age and site quality, and decade as a covariate (with value 1 to 7) to account for the trend with aging. This design accounted for the effect of repetitive measurements in each plot while expecting a linear monotonic relationship between variables and stand age. The relationship between AGB accumulation and mortality loss was analyzed with ANCOVA, in which AGB accumulation was used as a dependent variable, while plot and mortality were used as a main factor and covariate, respectively. The relationship between above-ground NPP and mortality (of individual or biomass loss) was analyzed with the same approach, with above-ground NPP as a dependent variable.

Results

Age-related decline of stand aboveground growth

For both stand chronosequence and long-term plots, total stand AGB increased with age with a reducing rate as stands aged (Fig. 1). Mean stand AGB as a function of age was well described using a quadratic equation (r^2>0.99), confirming an age-related decline of stand AGB accumulation.

Leaf physiology and chemistry

Most gas exchange parameters measured in this study displayed no significant differences among trees of different age classes, with the exception of *A* and R_N (Table 1). However, *A* did not decline with tree age as expected, and the age effect on R_N was attributed to the change in leaf nitrogen content (see below). The age effect on foliar A/R was not significant and the mean values of whole tree foliar photosynthesis/ wood respiration generally showed an increasing trend with age. Thus, these results did not support the prediction of H1-1 and H1-2 that *A* and *A*/*R* would decrease with tree age.

There was a significant age effect on leaf N_{mass}, and C/N, but the trend was opposite to the prediction of H1-3 that leaf nitrogen and C/N respectively decrease or increase with tree age; leaves from the youngest age class displayed lowest N_{mass} (and highest C/N) (Table 1). Although the difference in leaf protein concentration was significant among stands, the magnitude of this difference seemed too small (2.4%) to be biologically relevant.

Tree height peaked at *ca.* 24 meters and height growth was not substantial after 70 years. Huber values decreased with tree age, indicating hydraulic exacerbation. The leaf $\delta^{13}C$

showed no change among age classes, indicating unchanged water use efficiency (Table 1). These results provide a strong counter-argument for hydraulic limitation to carbon gain (H1-4).

Most observed physiological parameters showed seasonal fluctuation throughout 2003, but the effect of age and age × season were not significant for any parameter (see Appendix Table S3).

Tree growth

The AGB of individual trees and the annual growth rate of AGB per tree (1998–2002 average) all increased with age class (Table 1). After adjusting the growth rate with the total leaf area, the age effect became insignificant, indicating the growth efficiency was not different between the age classes.

The cross-dated tree ring width chronology indicated a decline in annual increment associated with age (Fig. 2a). It is evident that trees of different ages were incorporated into the chronology at different times (Fig. 2b). As individual trees possess a natural age-related decline in ring width (Fritts 1976), incorporation of trees of different ages into the chronology at different times will likely result in enhanced variability in ring width and underestimate the declining trend in time of the chronology. Subsequently, the actual decline in annual increment associated with age may be more significant than shown in Fig. 2a.

The relative growth rate decreased exponentially over the tree age (Fig. 2c). However, these declines did not offset the AGB accumulation (Fig. 2b) and annual AGB growth (Fig. 2c) of older trees. Overall, annual AGB growth increased through the first 130 years. Declining growth rates since the 1990s occurred in all four age classes (data not shown), so the trend

was mainly attributed to environmental conditions rather than age effect. Therefore, we reject H1-5 that the AGB growth of individual trees and growth efficiency decrease with age.

Canopy net carbon exchange

The four stands had similar *L* ranging between 2.0 and 2.4, suggesting canopy closure before or near 35 years of age. The fraction of the total leaf area of *Quercus* spp. in the canopy was also similar among the stands (73–79%). A_N ranged between 2.35 to 3.09 Mg C ha^{-1} (Table 2). In general, canopy carbon fluxes of *Quercus* (A_G, R_f, A_N) showed no clear trend associated with stand age, and R_f/A_G was generally constant (0.65–0.72). Parameters related to light use efficiency (α_{can}, Q_{can}, and ε_{can}) were also similar among these stands. Sensitivity analyses suggest that A_N was more sensitive to photosynthetic and respiratory parameters (V_{cmax}, J_{max}, R_0, E_0) than to *L* (see Appendix Fig. S2). Therefore, we reject H1-6 that canopy annual net foliar exchange decreases with stand age.

Stand growth dominance

Monitored trees in long-term plots constantly exhibited cumulative growth curves that were very close to the 1:1 line (Fig. 3a–g) and CGD close to 0 (-0.06–0.006) (Fig. 3h), suggesting no growth dominance throughout the 70-year time span. A generally consistent pattern was observed for individual plots, despite higher variability due to smaller sample size (data not shown). Therefore, we reject H2 that tree growth dominance would initially increase and subsequently decrease with stand development.

Stand aboveground biomass productivity

The above-ground NPP of the long-term plots ranged between 2950 and 4060 kg ha^{-1} yr^{-1} during the 70-year measurement span and appeared to be plot specific (plot effect P=0.004, ANCOVA). The absence of decade and plot × decade effects indicated a stable decadal status during 1937–2006 in all plots. The AGB accumulation in long-term plots generally decreased as stands aged (P=0.0003, ANCOVA, Fig. 4a). This trend was accompanied by increasing biomass loss due to mortality over time (P<0.0001, ANCOVA, Fig. 4a). Plot effects and plot by decade interactions were not significant for either of these two variables.

Stand AGB accumulation and mortality loss (two independently estimated variables) exhibited a negative linear relationship (P<0.0001, ANCOVA), with a coefficient close to -1 (-1.047, Fig. 4b), suggesting that AGB accumulation was predominantly determined by biomass loss due to mortality. This pattern appeared consistent among the plots (plot × mortality loss, P=0.83, ANCOVA). These results support H3-1: that mortality loss would increase with stand development while net above-ground productivity would be stable through time. Although the AGB accumulation and mortality displayed large temporal variability during 1987–2006, they generally fit the negative 1:1 relationship, and hence the variability does not counteract the overall pattern. In contrast, above-ground NPP was not correlated to annual mortality (P=0.73, ANCOVA) or mortality biomass loss (P=0.54) and the pattern was consistent among plots (P=0.80 for plot × annual mortality, P=0.83 for plot × mortality biomass loss, ANCOVA). This result, together with the constant above-ground NPP, does not support our H3-2 that age-related decline of stand biomass accumulation is mainly caused by increasing mortality-led NPP loss.

Mortality structure

The number of tree deaths in long-term plots decreased from about 30 trees ha^{-1} yr^{-1} in 1937–1946 to about 15 trees in 1997–2006; meanwhile, the annual mortality remained constant at about 2% without a clear decadal trend (1.8–2.4%; see Appendix Fig. S3a). At such low mortality rate, the exponential mortality coefficient was almost the same as annual mortality. The deviation of annual tree deaths, annual mortality and exponential mortality coefficient among plots (the ratio of standard error to mean) decreased during the first 20–30 years of the survey and remained relatively stable thereafter, indicating reduced variability regarding individual mortality rate as stands aged (see Appendix Fig. S3b).

The individual cumulative mortality curves were constantly far beyond the 1:1 line (Fig. 3a-g) with CMD-IND in the range of -0.65 to -0.89 without showing a clear temporal trend (Fig. 3h), indicating strong reverse dominance and limited changes in the structure of individual mortality (i.e. the distribution of dead trees over tree size was relatively constant) over time. In contrast, AGB mortality cumulative curves were beyond the 1:1 line during 1937–1976 (CMD-AGB =-0.3 to -0.4) but moved toward the 1:1 line during subsequent decades, and CMD-AGB increased to 0.02 during 1997–2006 (Fig. 3). These trends suggested that as stands aged, AGB mortality shifted from predominantly young, small trees to large, dominant trees. This shift in mortality was not due to an increase in the proportion of large trees that die, but rather because stands were composed of more large trees (indicated by increased average AGB of individual trees) and higher proportion of stand AGB were stored in larger trees that are subject to mortality loss over time (see Appendix Fig. S4). In other words, biomass loss increased because more large trees died, which is simply because there were more large trees in stands as stands aged.

Discussion

We found an age-related decline of stand AGB accumulation in a *Quercus*-dominated forest and examined three possible mechanisms. This decline was not likely to be caused by mechanisms that decreased above-ground NPP. We did not find evidence for reduced individual tree growth associated with age-related physiological constraints (decreased foliar/ canopy carbon fixation capacity and photosynthesis/ respiration balance, decreased nitrogen availability or increased hydraulic constraints on carbon gain), or alterations in stand structure that may reduce stand resource use efficiency, or increased mortality-led productivity loss. However, we found that increased biomass loss due to tree mortality was the primary cause of the age-related decline of stand AGB accumulation in the BRF. As stands aged, annual mortality and the structure of individual mortality did not change. In older stands with proportionately more large trees and fewer small trees, maintenance of the individual mortality rate and structure led to a shift of mortality AGB loss from small trees to large, dominant trees over time. As a result, the effect of tree mortality on AGB loss increased as stand age increased, and subsequently, the death of large trees was the primary mechanism driving age-related decline of stand biomass accumulation. This mechanism substantially explains age-related decline of stand biomass accumulation in the BRF during the first ~130 years of growth, which is typical of modern regenerating eastern deciduous forest in the United States. Additional studies would be required to examine whether the same mechanism applies to older forests of this type or whether different mechanisms shape age-related forest stand growth during the late stages of stand development.

Physiological constraints of tree growth and stand productivity decline

Age- or size-related decrease in growth of individual trees could decrease stand level productivity and thus lead to decline of forest biomass accumulation. Physiological constraints that may reduce the growth of older trees have been widely addressed, but few general insights have been gained. Resource-led (e.g. nutrient, water) physiological constraints on photosynthesis, which can reduce tree growth (see reviews of (Bond 2000; Niinemets 2002), appeared common, but increasing AGB growth in older trees has also been observed (Johnson & Abrams 2009; Sillett *et al.* 2010). Our study examined whether the growth of individual *Q. rubra* trees declined with age (H1-5) and tested hypotheses of potential physiological constraints: unbalanced carbon gain and respiration (H1-1, H1-2, H1-6), nutrient (nitrogen) limitation (H1-3), and hydraulic constraints (H1-4) (Gower, McMurtrie & Murty 1996). None of these hypotheses were supported for *Q. rubra* between 35–135 years old in the BRF, commensurate with observations of increasing basal area and biomass growth with increasing tree age in *Quercus* spp.(Schuster *et al.* 2008; Johnson & Abrams 2009), suggesting the pattern may be common for this important genus. Another potential physiological mechanism affecting the growth of older trees is the biomass allocation pattern, which was not tested in this study. High above-ground growth and growth efficiency of older trees observed in this study may be partially attributable to increasing biomass allocation to stems over time. Given the potential importance of biomass allocation, this should be addressed in further studies in the BRF.

Pioneering studies on forest stand development suggested that age-related decline of forest productivity was due to reduced photosynthesis to respiration ratios, primarily due to increased respiration over time. More recent empirical evidence rejected this hypothesis (Ryan, Binkley & Fownes 1997; Ryan *et al.* 2004); we also reject this hypothesis. Within the same stand chronosequence, a stand level model shows that the percentage of woody tissue respiration was relatively constant at 10% of GPP and was not affected by stand age (9.7,

11.8 and 10.6% of GPP respectively for 35-, 90-, and 135-year stands, Bowman 2005). In summary, responses of *Q. rubra* at the BRF are consistent with other studies, suggesting a minimal role for reduced photosynthesis and increased respiration as the cause of age-related decline of forest stand production.

Support for the nutrient and hydraulic limitation hypotheses is equivocal. In some cases, reduced nutrient availability may contribute to declining growth of older forests, but this response is not universal (Ryan, Binkley & Fownes 1997). Similarly, hydraulic limitation of gas exchange in taller (usually older) trees, although commonly observed, is not consistently supported (Ryan, Phillips & Bond 2006). In particular, the link between hydraulic limitation of carbon assimilation and tree growth is rarely studied (n.b. Barnard & Ryan 2003; Ryan *et al.* 2004). Therefore, these mechanisms for age-related forest stand productivity decline may be case-specific (e.g. species, season, and site). In our study, these two mechanisms did not limit individual tree growth of *Q. rubra* and forest NPP perhaps due to specific biological features of *Q. rubra*. For example, compared to more widely studied coniferous species, the relatively fast litter nutrient mobilization rate in *Quercus* forests may eliminate the nutrient limitation, as found in a study contrasting *Pinus sylvestris* and *Quercus robur* (Yuste *et al.* 2005). Furthermore, *Q. rubra* may adjust its growth pattern to alleviate hydraulic limitation. Hydraulic limitation has been suggested to be a function of tree size, especially tree height (Mencuccini *et al.* 2005; Martinez-Vilalta, Vanderklein & Mencuccini 2007; Abdul-Hamid & Mencuccini 2009), and support for the hydraulic limitation hypothesis has predominantly been observed in tall trees. In contrast, *Q. rubra* in this study shifted from vertical height growth to horizontal girth growth and crown expansion (data not shown) after 70 years. This transition in growth direction may minimize hydraulic limitation imposed by the length of the hydraulic path and gravitational potential. Similarly, *Quercus spp*. have a host of adaptations to drought such as waxy xeromorphic leaves, low water potential for stomatal closure, and

high photosynthetic rates in dry conditions which together may limit hydraulic constraints at the whole tree and stand level (Turnbull *et al.* 2001). More specifically, vessel elements in angiosperms such as *Q. rubra* are generally more specialized than tracheids in conifers for the efficient conduction of water (Hacke, Sperry & Pittermann 2005), yet much of the support for the hydraulic limitation hypothesis was obtained from coniferous stands (Ryan, Phillips & Bond 2006). Finally, nitrogen and hydraulic limitations may be moderated by nitrogen deposition and CO_2 fertilization (Phillips, Buckley & Tissue 2008) and the role of these stimulatory effects of global change phenomenon deserves further study.

Age-related stand structure change

Binkley *et al.* (2006) proposed a 4-phase dynamic of forest growth dominance and suggested the pattern plays a role in the age-related decline of forest productivity; this hypothesis has been tested and supported by a few studies (Binkley *et al.* 2002; Binkley 2004; Fernandez & Gyenge 2009). However, we did not observe growth dominance and its phase-switch during the past 70 years in the BRF. Although factors accounting for this sustained "evenness" in the relationship between tree size and growth are not clear, it is not entirely surprising because species-specific dynamics of dominance have been observed and similar patterns was shown in *Populus tremuloides* in the Rocky Mountains (Binkley *et al.* 2006). The cause of the phenomenon in *P. tremuloides* stands was attributed to clonal characteristics (Binkley *et al.* 2006), but this mechanism is not likely to apply to non-clonal, seed-reproduced oaks such as *Q. rubra* in BRF.

The absence of growth dominance in our observations may be related to the timing of dominance phase-switch. Binkley (2004) stated that growth dominance would occur just prior to canopy closure generating stand-level growth decline, while decline during further stand

development was attributed to the development of reverse dominance. However, there is limited information about the age at which these shifts occur and the length of the transition periods between phases. In *Eucalyptus saligna* monoculture plantations, the occurrence, peak, and offset of growth dominance was observed at 2, 10, and 20 years respectively (Binkley *et al.* 2003); in contrast, a reversal of growth dominance was not observed until >150 years for *Pinus contorta* stands (Binkley *et al.* 2006). Unfortunately, our long-term results do not cover the very young and very old stages of stand development, during which changes in stand structure may affect stand growth.

Increased mortality as a mechanism for age-related decline of stand biomass accumulation

Forest stand growth is the sum of above-ground NPP and mortality biomass loss. Therefore, decreased stand biomass accumulation may primarily be due to reduced NPP or to increased mortality biomass loss. Ryan, Binkley & Fownes (1997) concluded that reduced productivity rather than increased mortality was the cause of reduced net growth rate of older forest. This conclusion has been challenged by some more recent studies that observed mortality as a significant cause of age-related decline of stand biomass accumulation in conifer forests (Acker *et al.* 2002; Taylor & MacLean 2005). In this study, the constant above-ground NPP and negative 1:1 relationship between stand AGB accumulation and mortality loss indicated that age-related decline of stand AGB accumulation in the BRF was predominantly determined by increasing mortality loss rather than reduced above-ground NPP. Thus, the results in the BRF confirm that mortality could play an important role in generating age-related decline of stand biomass accumulation, primarily due to the loss of large, dominant trees.

In the BRF, relatively consistent above-ground NPP maintained the forest as a carbon sink over the past 70 years and we did not find any correlation between above-ground NPP and mortality, suggesting mortality-led loss of NPP did not significantly affect stand biomass accumulation. Two factors may contribute to the maintenance of above-ground NPP. First, old-growth forests can maintain productivity if they have sufficiently high tree densities (Luyssaert *et al.* 2008); tree density in BRF generally remained stable from the 70-year stand onward (see Appendix Table S1) or after 1950s in long-term plots (Schuster et al. 2008). Therefore, abundant new recruitments or growth of previously suppressed trees may compensate for the loss of productivity due to the mortality of older trees. Second, above-ground NPP may be stimulated by recent environmental changes so that the commonly observed age-related decline was negated (Boisvenue & Running 2006; Phillips, Buckley & Tissue 2008; McMahon, Parker & Miller 2010). In addition to elevated [CO_2], possible growth stimulating effects in BRF include a 1.0°C increase in mean air temperature over the 20^{th} century and a mean annual deposition of 6–7 kg N ha^{-1} (NADP 2007) . Further study of these factors may reveal their influence on wood NPP over time.

It is notable that the *Quercus*-dominated forest in the BRF exhibited high mortality rates during 1997–2006 (associated with droughts, see discussion below), in contrast to the low mortality in 1987–1996. This variability suggests that the observed mortality may be environmentally driven and therefore not solely age-related; however, this does not undermine our conclusion that age-related decline of stand AGB accumulation was predominantly driven by mortality loss. Overall, the mortality and stand AGB accumulation of these two decades still adhere to the general 1:1 negative relationship that fits the entire survey record (i.e. for 1987–1996, high stand AGB accumulation was primarily due to low mortality and *vice versa* for 1997–2006). Interestingly, mortality may function very differently from the broadly studied and accepted physiological constraints on NPP in terms

of shaping forest stand biomass accumulation. The influence of age- or size- related physiological constraints on NPP may have inherently low variability because age and size increment in trees are continual and irreversible. Furthermore, the influence of physiological variability on NPP is ultimately limited by maximum potential tree growth, which is < 2% of the whole tree biomass of large trees (Fig. 2c). By contrast, tree mortality acts as a cumulative probability over time and is subject to environmental and stochastic factors. In particular, for older forests, a considerable proportion of biomass would exist in a small number of large, dominant trees and death events that have high impact on stand growth would only happen intermittently. Such inherent stochastic behaviour suggests that mortality as a mechanism to reduce biomass accumulation of forest stands must be evaluated using long-term trend analyses because shorter-term studies may easily be biased by intermittent events. Subsequently, the covariance between mortality and stand growth should be emphasized as well as the temporal trend.

As forests age, the major cause of tree mortality shifts from competition for resources to aging and exposure to disturbances (Taylor & MacLean 2005). In contrast to some physiological growth models (sigmoidal growth of individual tree), increasing growth of individual trees has been observed in old-growth *Quercus* and other common tree species in the eastern US (Johnson & Abrams 2009); our results of tree-ring analysis and allometric estimation of tree biomass in the chronosequence plots support these observations. Therefore, we postulate that for these species like *Q. rubra*, tree mortality associated with size-related exposure to disturbances, rather than reduced growth of individual trees over time, can generate forest stand biomass accumulation decline over time. In addition, significant disturbance-driven tree mortality may happen before physiological/ genetic constraints on growth occur and thus shape the stand AGB accumulation. In *Abies* and *Picea* forests in New Brunswick, Canada, mortality was indicated as the major reason for stand decline with more

than 60% due to wind-throw, stem- or top-breakage and insects (Taylor & MacLean 2005). In the BRF, periods of slower or negative stand AGB accumulation were also associated with insect outbreaks and droughts (Schuster *et al.* 2008). The variability of mortality observed during the 1987–2006 time period may be related to the favourable decade of 1987–1996 followed by several significant droughts since 1999, accompanied by substantial tree death during 1999–2005 (Schuster *et al.* 2008). It is notable that disturbances are subject to many stochastic factors and their frequency and intensity has large temporal and spatial variability. Stochastic disturbance events make the influence of mortality on forest productivity significantly more difficult to detect (Foster *et al.* 2010). Compared with deaths of seedlings and small trees, disturbance-driven deaths of dominant trees are rare, variable, high-impact events, whose variability simply cannot be incorporated into chronosequence studies and would confound surveys with insufficient time spans. For example, in our study no clear trends in stand growth or the relationship between mortality and stand growth decline would be observed based on observations during any 20- to 30-year period.

In northern temperate forests, the rate of change in tree biomass and the factors generating that change are of primary importance in assessing current and near-future carbon stocks (Houghton 2005). To predict the change of carbon stock in old-growth forests with mortality as a primary determinant of stand biomass accumulation, we suggest that model studies include tree demography, as well as the influence of stochastic factors and climate change on disturbances that are associated with tree death. For example, climate models project increasing frequency and/or intensity of disturbances, such as fire, pest and disease outbreak, and extreme weather events in some regions (Easterling *et al.* 2007). These factors are likely to increase tree mortality and thus decrease carbon stock in above-ground biomass of older forests, but have not been well modelled. Future studies on these topics will improve our capability to infer forest living biomass as carbon sources or sinks in the terrestrial biosphere.

Acknowledgement

This study was supported by a Black Rock Forest small grant funded by the Ernst C. Stiefel Foundation. We also thank N. Pederson for the assistance on tree age information at the BRF. We also thank the associate editor and two reviewers' critical comments that improved the manuscript.

References

Abdul-Hamid, H. & Mencuccini, M. (2009) Age- and size-related changes in physiological characteristics and chemical composition of *Acer pseudoplatanus* and *Fraxinus excelsior* trees. *Tree Physiology*, **29,** 27-38.

Acker, S.A., Halpern, C.B., Harmon, M.E. & Dyrness, C.T. (2002) Trends in bole biomass accumulation, net primary production and tree mortality in *Pseudotsuga menziesii* forests of contrasting age. *Tree Physiology*, **22,** 213-217.

Barnard, H.R. & Ryan, M.G. (2003) A test of the hydraulic limitation hypothesis in fast-growing *Eucalyptus saligna*. *Plant Cell and Environment,* **26,** 1235-1245.

Berger, U., Hildenbrandt, H. & Grimm, V. (2004) Age-related decline in forest production: modelling the effects of growth limitation, neighbourhood competition and self-thinning. *Journal of Ecology*, **92,** 846-853.

Binkley, D. (2004) A hypothesis about the interaction of tree dominance and stand production through stand development. *Forest Ecology and Management,* **190,** 265-271.

Binkley, D. & Arthur, M. (1993) How to count dead trees. *Bulletin of the Ecological Society of America*, **74,** 15-16.

Binkley, D. & Greene, S. (1983) Production in mixtures of conifers and red alder: the importance of site fertility and stand age. *IUFRO symposium on forest site and continuous productivity. Seattle, Washington, August 22-28, 1982* (eds R. Ballard & S.P. Gessel), pp. 112-117. General Technical Report, Pacific Northwest Forest and Range Experiment Station, USDA Forest Service, Portland, OR, USA.

Binkley, D., Kashian, D.M., Boyden, S., Kaye, M.W., Bradford, J.B., Arthur, M.A., Fornwalt, P.J. & Ryan, M.G. (2006) Patterns of growth dominance in forests of the Rocky Mountains, USA. *Forest Ecology and Management*, **236,** 193-201.

Binkley, D., Senock, R.S., Bird, S. & Coles, T.G. (2003) Twenty years of stand development in pure and mixed stands of *Eucalyptus saligna* and nitrogen-fixing *Facaltaria mollucana*. *Forest Ecology and Management*, **182,** 93-102.

Binkley, D., Stape, J.L., Ryan, M.G., Barnard, H.R. & Fownes, J. (2002) Age-related decline in forest ecosystem growth: An individual-tree, stand-structure hypothesis. *Ecosystems*, **5,** 58-67.

Boisvenue, C. & Running, S.W. (2006) Impacts of climate change on natural forest productivity - evidence since the middle of the 20th century. *Global Change Biology*, **12,** 862-882.

Bond, B.J. (2000) Age-related changes in photosynthesis of woody plants. *Trends in Plant Science*, **5,** 349-353.

Bowman, W.P. (2005) Respiratory ecophysiology of woody stems and branches in temperate forest trees. Ph. D., Columbia University.

Brenneman, B.B., Frederick, D.J., Gardner, W.E., Schoenhofen, L.H. & Marsh, P.L. (1978) Biomass of species and stands of West Virginia hardwoods. *Proceedings of central hardwood forest conference II.* (ed. P.E. Pope), pp. 159-178. Purdue University, West LaFayette, IN.

Cooper, C.F. (1983) Carbon storage in managed forests. *Canadian Journal of Forest Research-Revue Canadienne De Recherche Forestiere,* **13,** 155-166.

DeBell, D.S. & Franklin, J.F. (1987) Old-growth Douglas-fir and western hemlock: a 36-year record of growth and mortality. *Western Journal of Applied Forestry,* **2,** 111-114.

Easterling, W.E., Aggarwal, P.K., Batima, P., Brander, K.M., Erda, L., Howden, S.M., Kirilenko, A., Morton, J., Saoussana, J.F., Schmidhuber, J. & Tubiello, F.N. (2007) Food, fibre and forest products. *Climate change 2007: impacts, adaptation,a nd vulnerability. Contribution of working group II to the fourth assessment report of the intergovernmental panel on climate change* (eds M.L. Parry, O.F. Canziani, J.P. Palutikof, P.J. van der Linden & C.E. Hanson), pp. 273-313. Cambridge University Press, Cambridge, UK.

Farquhar, G.D., Caemmerer, S.V. & Berry, J.A. (1980) A biochemical-model of photosynthetic CO_2 assimilation in leaves of C_3 species. *Planta,* **149,** 78-90.

Fernandez, M.E. & Gyenge, J. (2009) Testing Binkley's hypothesis about the interaction of individual tree water use efficiency and growth efficiency with dominance patterns in open and close canopy stands. *Forest Ecology and Management,* **257,** 1859-1865.

Foster, J.R., Burton, J.I., Forrester, J.A., Liu, F., Muss, J.D., Sabatini, F.M., Scheller, R.M. & Mladenoff, D.J. (2010) Evidence for a recent increase in forest growth is questionable. *Proceedings of the National Academy of Sciences,* **107,** E86-E87.

Fritts, H.C. (1976) *Tree rings and climate*. Academic Press, London.

Gower, S.T., McMurtrie, R.E. & Murty, D. (1996) Aboveground net primary production decline with stand age: Potential causes. *Trends in Ecology & Evolution,* **11,** 378-382.

Grier, C.C., Lee, K.M., Nadkarni, N.M., Klock, G.O. & Edgerton, P.J. (1989) Productivity of forests of the United States and its relation to soil and site factors and management

practices: a review. *General Technical Report - Pacific Northwest Research Station, USDA Forest Service*.

Grier, C.C. & Logan, R.S. (1977) Old-growth *Pseudotsuga-menziesii* communities of a western oregon watershed - biomass distribution and production budgets. *Ecological Monographs,* **47,** 373-400.

Hacke, U.G., Sperry, J.S. & Pittermann, J. (2005) Efficiency vs. safety trade-offs for water conduction in angiosperm vessels vs. gymnosperm tracheids. *Vascular transport in plants* (eds N.M. Holbrook & M. Zwieniecki), pp. 333-353. Elsevier, Amsterdan, Netherland.

Hocker, H.W. & Earley, D.J. (1983) Biomass and leaf area equations for northern forest species. *Research report - agricultural experiment station, University of New Hampshire,* **102,** 27.

Houghton, R.A. (2005) Aboveground forest biomass and the global carbon balance. *Global Change Biology,* **11,** 945-958.

Hurtt, G.C., Pacala, S.W., Moorcroft, P.R., Caspersen, J., Shevliakova, E., Houghton, R.A. & Moore, B. (2002) Projecting the future of the US carbon sink. *Proceedings of the National Academy of Sciences of the United States of America,* **99,** 1389-1394.

Johnson, S.E. & Abrams, M.D. (2009) Age class, longevity and growth rate relationships: protracted growth increases in old trees in the eastern United States. *Tree Physiology,* **29,** 1317-1328.

Martinez-Vilalta, J., Vanderklein, D. & Mencuccini, M. (2007) Tree height and age-related decline in growth in Scots pine (*Pinus sylvestris* L.). *Oecologia,* **150,** 529-544.

McMahon, S.M., Parker, G.G. & Miller, D.R. (2010) Evidence for a recent increase in forest growth. *Proceedings of the National Academy of Sciences,* **107,** 3611-3615.

Mencuccini, M., Martinez-Vilalta, J., Vanderklein, D., Hamid, H.A., Korakaki, E., Lee, S. & Michiels, B. (2005) Size-mediated ageing reduces vigour in trees. *Ecology Letters,* **8,** 1183-1190.

Monteith, D.B. (1979) Whole-tree weight tables for New York. *AFRI Research Report 40*, pp. 40.

NADP (2007) National atmospheric deposition program 2006 annual summary. *NADP data report 2007-01*, pp. 16. NADP program offfice, Champaign, IL.

Niinemets, U. (2002) Stomatal conductance alone does not explain the decline in foliar photosynthetic rates with increasing tree age and size in *Picea abies* and *Pinus sylvestris*. *Tree Physiology,* **22,** 515-535.

Phillips, N.G., Buckley, T.N. & Tissue, D.T. (2008) Capacity of old trees to respond to environmental change. *Journal of Integrative Plant Biology,* **50,** 1355-1364.

Ryan, M.G., Binkley, D. & Fownes, J.H. (1997) Age-related decline in forest productivity: pattern and process. *Advances in Ecological Research, Vol 27*, pp. 213-262. Academic Press Ltd, London.

Ryan, M.G., Binkley, D., Fownes, J.H., Giardina, C.P. & Senock, R.S. (2004) An experimental test of the causes of forest growth decline with stand age. *Ecological Monographs,* **74,** 393-414.

Ryan, M.G., Phillips, N. & Bond, B.J. (2006) The hydraulic limitation hypothesis revisited. *Plant Cell and Environment,* **29,** 367-381.

Schuster, W.S.F., Griffin, K.L., Roth, K., Turnbull, M.H., Whitehead, D. & Tissue, D.T. (2008) Changes in composition, structure and aboveground biomass over seventy-six years (1930-2006) in the Black Rock Forest, Hudson Highlands, southeastern New York State. *Tree Physiology,* **28,** 537-549.

Sheil, D., Burslem, D.F.R.P. & Alder, D. (1995) The interpretation and misinterpretation of mortality-rate measures. *Journal of Ecology,* **83,** 331-333.

Sillett, S.C., Van Pelt, R., Koch, G.W., Ambrose, A.R., Carroll, A.L., Antoine, M.E. & Mifsud, B.M. (2010) Increasing wood production through old age in tall trees. *Forest Ecology and Management,* **259,** 976-994.

Smith, F.W. & Long, J.N. (2001) Age-related decline in forest growth: an emergent property. *Forest Ecology and Management,* **144,** 175-181.

Taylor, S.L. & MacLean, D.A. (2005) Rate and causes of decline of mature and overmature balsam fir and spruce stands in New Brunswick, Canada. *Canadian Journal of Forest Research-Revue Canadienne De Recherche Forestiere,* **35,** 2479-2490.

Turnbull, M.H., Whitehead, D., Tissue, D.T., Schuster, W.S.F., Brown, K.J. & Griffin, K.L. (2001) Responses of leaf respiration to temperature and leaf characteristics in three deciduous tree species vary with site water availability. *Tree Physiology,* **21,** 571-578.

Turner, J. & Long, J.N. (1975) Accumulation of organic matter in a series of Douglas-Fir stands. *Canadian Journal of Forest Research,* **5,** 681-690.

Tyree, M.T. & Ewers, F.W. (1991) The hydraulic architecture of trees and other woody-plants. *New Phytologist,* **119,** 345-360.

Weiner, J. & Thomas, S.C. (2001) The nature of tree growth and the "age-related decline in forest productivity". *Oikos,* **94,** 374-376.

Whitehead, D., Griffin, K.L., Turnbull, M.H., Tissue, D.T., Engel, V.C., Brown, K.J., Schuster, W.S.F. & Walcroft, A.S. (2004a) Response of total night-time respiration to differences in total daily photosynthesis for leaves in a *Quercus rubra* L. canopy: implications for modelling canopy CO_2 exchange. *Global Change Biology,* **10,** 925-938.

Whitehead, D., Walcroft, A.S., Griffin, K.L., Tissue, D.T., Turnbull, M.H., Engel, V.C., Brown, K.J. & Schuster, W.S.F. (2004b) Scaling carbon uptake from leaves to canopies: insights from two forest with contrasting properties. *Forests at the land-atmosphere interface* (eds M. Mencuccini, J. Grace, J. Moncrieff & K.G. McNaughton), pp. 231-254. CABI Publishing, Wallingford, UK.

Yuste, J.C., Konopka, B., Janssens, I.A., Coenen, K., Xiao, C.W. & Ceulemans, R. (2005) Contrasting net primary productivity and carbon distribution between neighboring stands of *Quercus robur* and *Pinus sylvestris*. *Tree Physiology*, **25,** 701-712.

Appendices:

Methods

Table 1. Tree age effect on physiological parameters and leaf characteristics of upper canopy leaves. Values shown are means ± (SE). ANOVA results (*P*-values) are shown and means are compared by LSD for variables with significant age effect (*P*<0.05 in **bold font**) and values followed by the same letter are not significantly different.

Parameters	Age stage and mean tree age (year)				*P* (ANOVA)
	35-year 36.8 (0.6) (n=12)	70-year 68.8 (0.6) (n=12)	90-year 91.4 (0.7) (n=23)	135-year 136.8 (1.9) (n=13)	
Photosynthesis and respiration					
V_{cmax} (20 °C, μmol m^{-2} s^{-1})	38.8(3.6)	29.8(3.2)	32.7(2.5)	36.2(4.8)	0.19
J_{max} (20 °C, μmol m^{-2} s^{-1})	75.8(6.8)	58.7(4.9)	62.7(4.0)	79.7(6.8)	0.06
A (20 °C, μmol m^{-2} s^{-1})	11.1(1.1)^{b}	7.4(0.8)^{a}	8.4(0.7)^{ab}	9.4(0.8)^{ab}	**0.03**
A_{mass} (20 °C, μmol kg^{-1} s^{-1})	134(15)	91.8(10.3)	105.5(8.8)	108.7(8.4)	0.19
PNUE (20 °C, μmol gN^{-1} s^{-1})	6.8(0.8)	3.7(0.4)	4.4(0.4)	4.6(0.4)	0.07
Rubisco activity (μmol m^{-2} s^{-1})	11.7(1.3)	12.9(0.9)	13.4(0.7)	13.6(0.8)	0.68
Q_{10} (15-25 °C)	1.98(0.09)	2.07(0.07)	2.12(0.08)	2.04(0.15)	0.76
E_0 (kJ mol^{-1})	48.3(2.9)	51.4(2.2)	52.7(2.5)	49.4(4.5)	0.71
$R_{0\ area}$ (10 °C, μmol m^{-2} s^{-1})	0.79(0.08)	0.7(0.06)	0.69(0.05)	0.77(0.06)	0.60
$R_{0\ mass}$ (10 °C, μmol kg^{-1} s^{-1})	9.1(1.0)	8.7(0.7)	8.4(0.6)	8.9(0.8)	0.91
$R_{0\ N}$ (10 °C, μmol gN^{-1} s^{-1})	0.45(0.05)	0.34(0.02)	0.35(0.02)	0.38(0.04)	0.07
R_{area} (20 °C, μmol m^{-2} s^{-1})	1.54(0.12)	1.46(0.11)	1.42(0.07)	1.52(0.06)	0.72
R_{mass} (20 °C, μmol kg^{-1} s^{-1})	18(1.5)	18.2(1.2)	17.5(0.8)	17.8(1.0)	0.96
R_N (20 °C, μmol gN^{-1} s^{-1})	0.89(0.07)^{b}	0.70(0.03)^{a}	0.72(0.04)^{a}	0.75(0.04)^{ab}	**0.05**
A/R (20 °C, area)	7.7(1.4)	5.5(0.8)	6.0(0.5)	6.1(0.4)	0.32
A/R (20 °C, whole tree)*	36.1(12.4)	--	42.0(12.1)	199.0(89.7)	--
Nitrogen and protein					
N_{area} (g m^{-2})	1.77(0.11)	2.08(0.08)	1.98(0.07)	2.06(0.08)	0.18
N_{mass} (%)	2.06(0.1)^{a}	2.55(0.08)^{b}	2.43(0.05)^{b}	2.38(0.05)^{ab}	**<0.001**
C/N (g g^{-1})	28.4(1.2)^{b}	23.3(0.6)^{a}	24.0(0.4)^{a}	24.8(0.5)^{a}	**<0.001**
Protein (mg ml^{-1})	58.2(0.1)^{a}	59.6(0.1)^{b}	59.2(0.2)^{ab}	58.3(0.3)^{a}	**<0.001**
Hydraulic limitation					
Tree height (m)	14.4(0.7)^{a}	23.3(0.8)^{bc}	20.5(0.7)^{b}	24.0(1.0)^{c}	**<0.001**
Huber value (cm^2m^{-2})	0.180(0.017)^{c}	0.103(0.009)^{b}	0.094(0.009)^{b}	0.060(0.009)^{a}	**<0.001**
$\delta^{13}C$ (‰)	-26.5(0.2)	-26.1(0.1)	-26.4(0.1)	-26.6(0.1)	0.34
Aboveground growth					
Total aboveground biomass (kg)	96(14)^{a}	447(38)^{b}	772(68)^{c}	2405(222)^{d}	**<0.001**
Growth 98-02 (kg yr^{-1})	3.6(0.5)^{a}	11.0(1.8)^{b}	16.4(1.8)^{b}	27.6(2.3)^{c}	**<0.001**
Growth per leaf area 98-02 (g m^{-2} yr^{-1})	85.8(8.0)	68.7(8.5)	70.8(7.3)	56.3(5.0)	0.14

*Calculated as (A × total leaf area of the tree)/(stem CO_2 efflux rate × trunk area of the tree) with area based stem CO_2 efflux rate from (Bowman 2005). ANOVA was not done because only mean and error were reported for stem CO_2 efflux. Standard error in the table was calculated with the approach of error analysis.

Table 2. Leaf area index, canopy composition, and canopy carbon flux model results (carbon fluxes and light use efficiency) of four stands with different age. Values shown are mean ± (SE).

Canopy info. or model results	Stand			
	35-year	70-year	90-year	135-year
L (canopy photo, n=12)	2.16 (0.11)	2.05 (0.07)	2.44 (0.11)	2.36 (0.09)
f_Q (%)	78.7	73.6	76.2	73.2
A_G (Mg C ha^{-1})	9.01	7.53	8.56	8.38
R_f (Mg C ha^{-1})	5.92	5.18	6.16	5.78
R_f/A_G	0.66	0.69	0.72	0.69
A_N (Mg C ha^{-1})	3.09	2.35	2.40	2.60
α_{can} (mol C mol^{-1} PAR)	0.0360	0.0357	0.0374	0.0359
Q_{can} (%)	62	62	62	61
ε_{can} (mol C mol^{-1} Q)	0.0156	0.0140	0.0152	0.0159

Figure legends:

Figure 1. Map of the Black Rock Forest (BRF) and the aboveground biomass of studied plots. a: map of the BRF showing long-term plots (numbered squares) and stand chronosequence plots (marked with letters). b: above-ground biomass of *Quercus rubra*, other *Quercus* spp. and other tree species are shown for four stand chronosequence plots in 2006. c: decadal average of above-ground biomass of *Quercus* spp. and other tree species in eight long-term plots during 1937–2006. The proportion of above-ground biomass (%) is marked for each composition. Error bars indicate the standard error of total aboveground biomass (n=2 for stand chronosequence plots and n=8 for long-term plots). The total above-ground biomass is fitted with a quadratic curve to show the age-related, declining trend (R^2>0.99).

Figure 2. Tree ring width chronology and above-ground growth. a: thin solid line, the average raw tree ring width; bold solid line, 11 year moving average; bold dashed line, long term tree ring width growth trend (equation and R^2 are shown). b: sample depth (thin solid line) of tree ring width data and above-ground biomass accumulation trajectory (bold solid line) calculated based on tree ring width chronology and allometric relationship. c: annual above-ground growth (solid line) and relative growth rate (dashed line) of the studied trees in the oldest plot. The bold solid line shows 11 year moving average of annual above-ground growth.

Figure 3. Growth and mortality dominance of all monitored trees in long-term plots (1937–2006). The dominance curve (a–g) plots the cumulative increment distribution of above-ground growth or mortality (y) as a function of the cumulative above-ground biomass distribution (x). The coefficient of growth dominance (CGD, solid line) and mortality dominance of above-ground biomass (CMD-AGB, dashed line) and individuals (CMD-IND,

dotted line) are shown for each decade (a–g) and summarized in j. The 1:1 and coefficient of dominance=1 lines are shown in grey solid line for reference.

Figure 4. Annual average of stand AGB accumulation, mortality loss and aboveground NPP of each decade during 1937–2006 are shown (a). Aboveground NPP and mortality loss are respectively presented in white and grey vertical bars as mean ± SE. Stand AGB accumulation is shown by the solid circle (mean ± SE). ANCOVA results (*P* values) are shown for the effect of plot, decade, and plot × decade. The relationship between stand AGB accumulation and mortality loss are shown for each plot (b). ANCOVA results (*P* values) are shown for the effect of plot, mortality (covariate) and plot × mortality.

Figure 1.

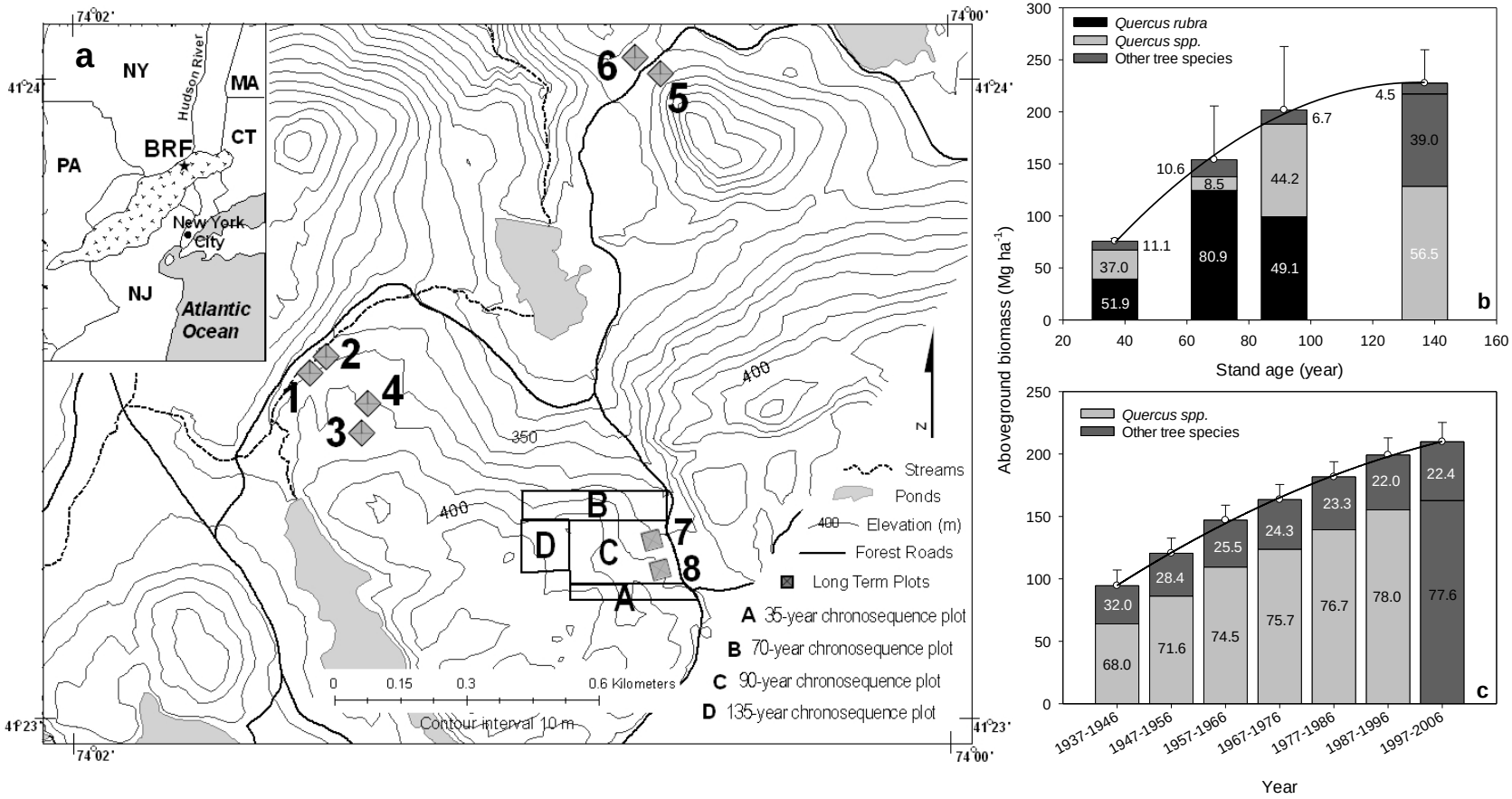
a
NY
MA
CT
PA
BRF
Hudson River
New York City
NJ
Atlantic Ocean
74°02'
74°00'
41°24'
41°23'
1
2
3
4
5
6
7
8
A
B
C
D
350
400
N
Streams
Ponds
Elevation (m)
Forest Roads
Long Term Plots
A 35-year chronosequence plot
B 70-year chronosequence plot
C 90-year chronosequence plot
D 135-year chronosequence plot
0 0.15 0.3 0.6 Kilometers
Contour interval 10 m
Quercus rubra
Quercus spp.
Other tree species
Aboveground biomass (Mg ha-1)
Stand age (year)
b
11.1
37.0
51.9
10.6
8.5
80.9
6.7
44.2
49.1
4.5
39.0
56.5
Quercus spp.
Other tree species
c
Year
1937-1946
1947-1956
1957-1966
1967-1976
1977-1986
1987-1996
1997-2006
32.0
68.0
28.4
71.6
25.5
74.5
24.3
75.7
23.3
76.7
22.0
78.0
22.4
77.6

Figure 2.

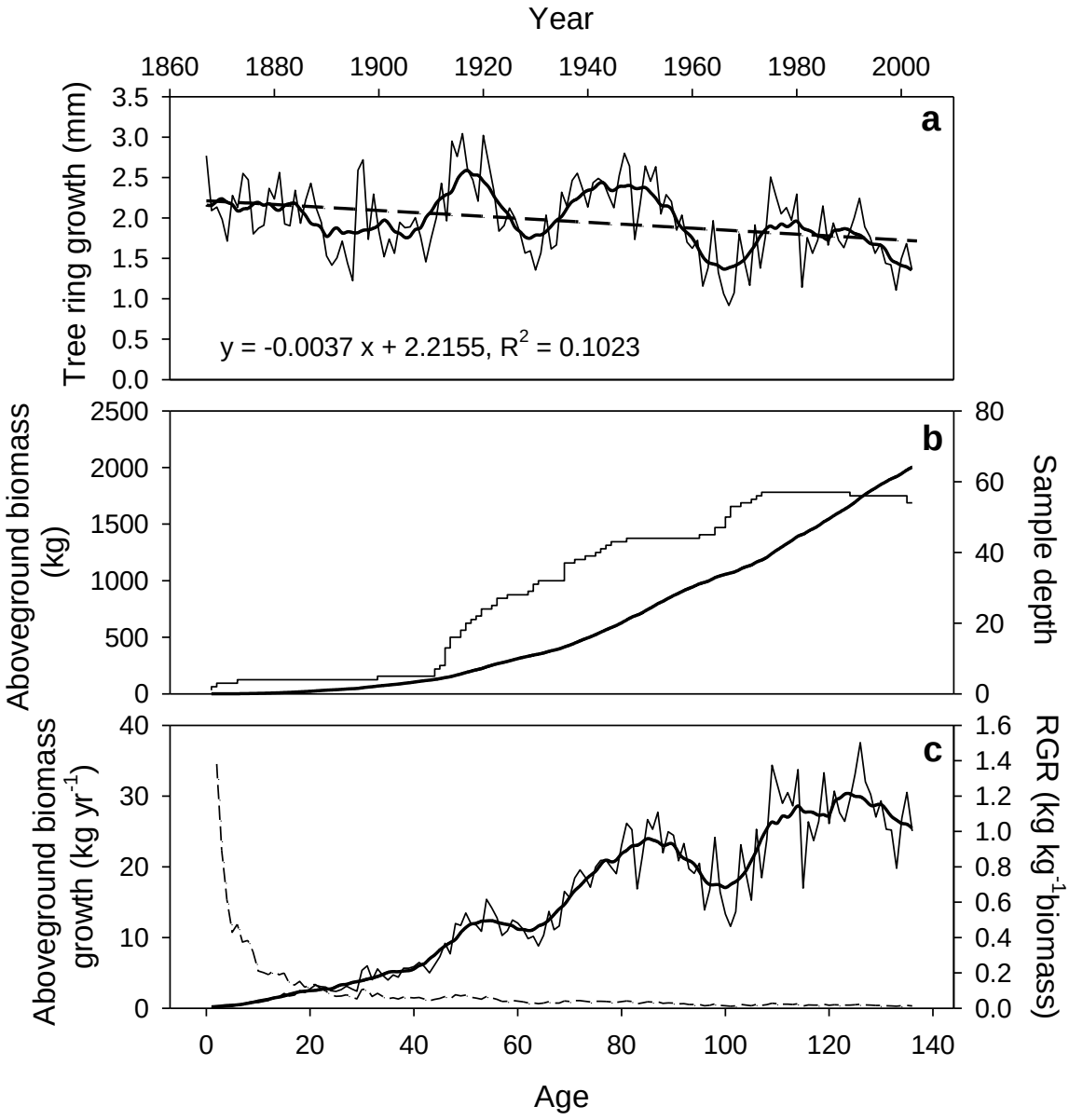
Year
1860
1880
1900
1920
1940
1960
1980
2000
Tree ring growth (mm)
a
y = -0.0037 x + 2.2155, R2 = 0.1023
Aboveground biomass (kg)
b
Sample depth
Aboveground biomass growth (kg yr-1)
c
RGR (kg kg-1biomass)
Age

Figure 3.

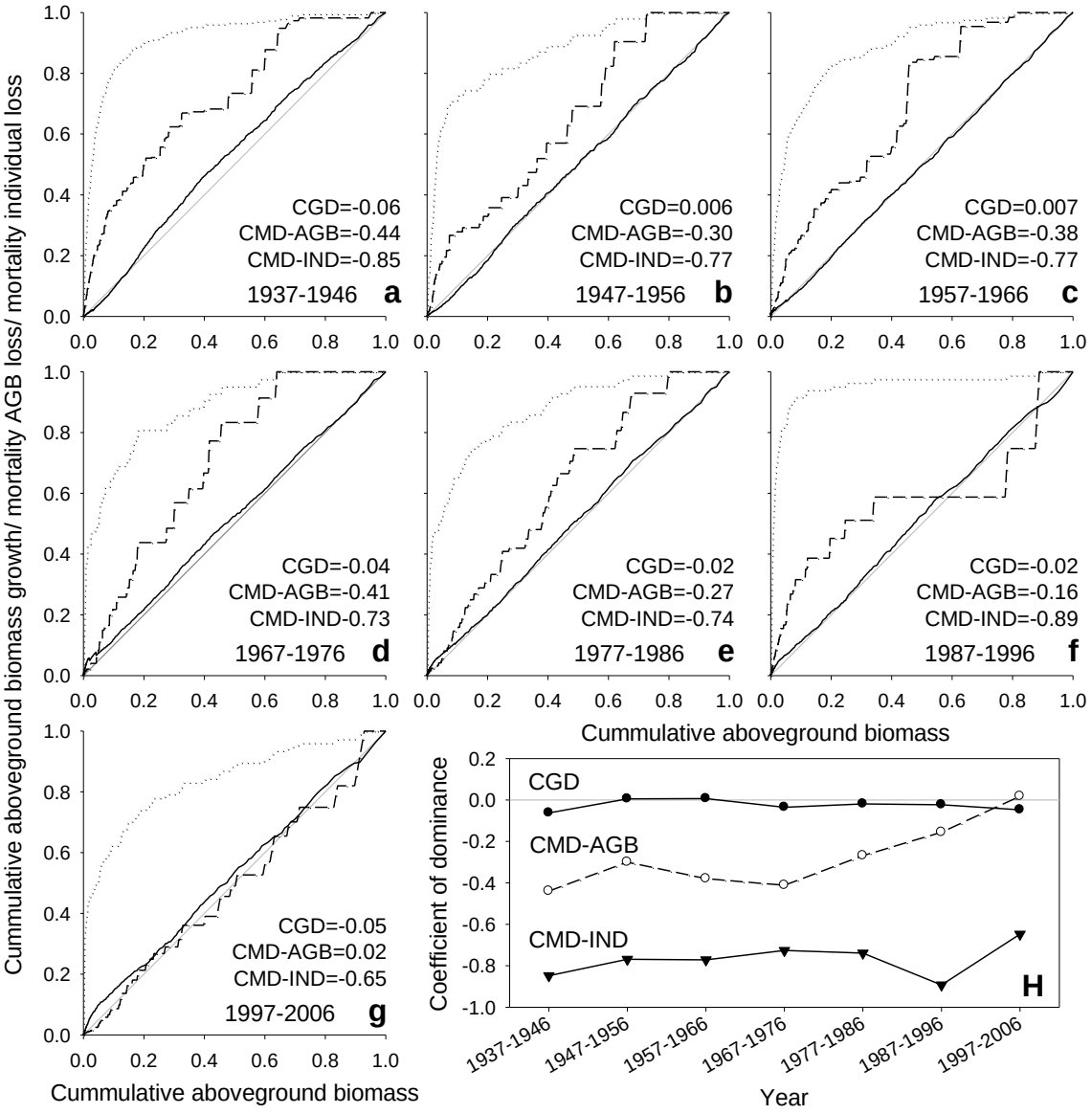
Cummulative aboveground biomass growth/ mortality AGB loss/ mortality individual loss
CGD=-0.06
CMD-AGB=-0.44
CMD-IND=-0.85
1937-1946 a
CGD=0.006
CMD-AGB=-0.30
CMD-IND=-0.77
1947-1956 b
CGD=0.007
CMD-AGB=-0.38
CMD-IND=-0.77
1957-1966 c
CGD=-0.04
CMD-AGB=-0.41
CMD-IND-0.73
1967-1976 d
CGD=-0.02
CMD-AGB=-0.27
CMD-IND=-0.74
1977-1986 e
CGD=-0.02
CMD-AGB=-0.16
CMD-IND=-0.89
1987-1996 f
CGD=-0.05
CMD-AGB=0.02
CMD-IND=-0.65
1997-2006 g
Cummulative aboveground biomass
Cummulative aboveground biomass
CGD
CMD-AGB
CMD-IND
H
Coefficient of dominance
1937-1946
1947-1956
1957-1966
1967-1976
1977-1986
1987-1996
1997-2006
Year

Figure 4.

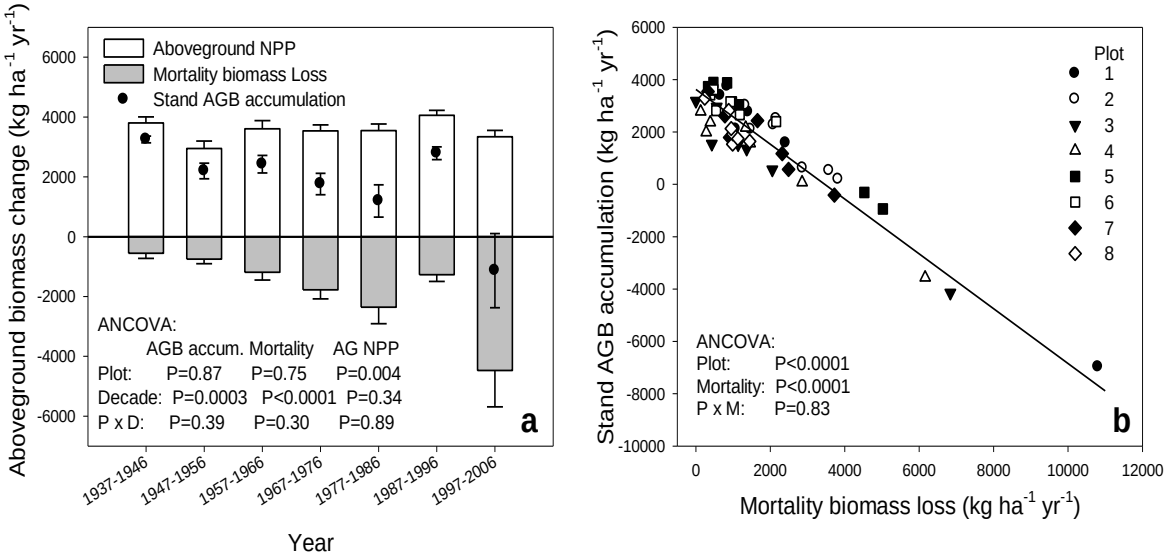
Aboveground NPP
Mortality biomass Loss
Stand AGB accumulation
ANCOVA:
AGB accum. Mortality AG NPP
Plot: P=0.87 P=0.75 P=0.004
Decade: P=0.0003 P<0.0001 P=0.34
P x D: P=0.39 P=0.30 P=0.89
a
Aboveground biomass change (kg ha-1 yr-1)
6000
4000
2000
0
-2000
-4000
-6000
1937-1946
1947-1956
1957-1966
1967-1976
1977-1986
1987-1996
1997-2006
Year
Plot
1
2
3
4
5
6
7
8
ANCOVA:
Plot: P<0.0001
Mortality: P<0.0001
P x M: P=0.83
b
Stand AGB accumulation (kg ha-1 yr-1)
6000
4000
2000
0
-2000
-4000
-6000
-8000
-10000
0
2000
4000
6000
8000
10000
12000
Mortality biomass loss (kg ha-1 yr-1)

Appendices

Methods

Site conditions

The topography of the Black Rock Forest (BRF) is rocky with steep slopes. Elevations in the forest range from 110 – 450 m above sea level with average seasonal temperatures from –2.7˚C in January to 23.4˚C in July. The soils are acidic and are mostly medium texture loams. Soil of the forest is typically very thin with bedrock or glacial till, ranging from 10-15 cm in upland areas to greater than 1 m in depressed areas. The nutrient availability of BRF is low and site index ranges from poor to good. There are approximately 735 trees per hectare throughout the forest with an average basal area of 29.0 m^2 ha^{-1} in the last large scale forest survey (Schuster *et al.* 2008). Red oak (*Quercus rubra*), Chestnut oak (*Q. prinus*) and Red maple (*Acer rubrum*) are the three most dominant species, respectively representing 42.3%, 23.8%, and 7.6% of the total basal area. The forest has functioned as a carbon sink for most of the 20th century (Schuster *et al.* 2008). Unregulated timber extraction from the forest ceased in 1928 (Tryon 1930), when the BRF was established as a forest research facility and records of all treatments have been maintained since then.

Studied plots

We selected adjacent *Q. rubra* dominated stands with 4 distinct age classes (approximately 35-, 70-, 90-, and 135-years since the last clear cutting). Within each stand, two 0.04 ha subplots were surveyed in 2006 for all trees with diameter at breast height (1.3m, *D*) larger than 2.54 cm. The eight long-term plots, ranging in size from 0.04 to 0.1 ha, were established between 1931 and 1936 to monitor forest growth (Tryon 1939, Fig. 1a) and are generally typical of the forest in composition and aboveground biomass (ABG). The details were reported in Schuster *et al.* (2008). They were surveyed at intervals ranging from 3 to 10 years before 1994 and then yearly since 1994. All trees with *D* larger than 2.54 cm were recorded and tracked until their death.

Gas exchange measurement

Sunlit upper canopy branches were detached using a shotgun in early morning. The branches were immediately excised under water and carried back to the laboratory for measurements. One mature, intact leaf was selected from each tree for photosynthesis and respiration measurements. Previous studies had shown no differences in photosynthesis and respiration between *in situ* leaves and leaves from detached branches in *Q. rubra* (Mitchell et al. 1999) and we confirmed that finding at our research site (Turnbull and Griffin, unpublished data).

Gas exchange measurements were made with infrared gas analysis systems (LI-6400, Li-Cor, Inc., Lincoln NE) equipped with CO_2 and temperature control modules. *A*-C_i curves were generated for each selected leaf at room temperature (22 – 27 °C). External CO_2

partial pressure (C_a) was set to 10 or 11 levels between 10 and 200 Pa. At each C_a set point, photosynthetic parameters were recorded when gas exchange had equilibrated (taken to be when the coefficient of variation for C_a between the sample and reference analyser was below 1%), which typically took 1-2 minutes to achieve. A constant, saturating photosynthetic photon flux density (1500 µmol m^{-2} s^{-2} PPFD) was supplied by blue-red light-emitting diodes mounted above the leaf cuvette. Respiration rates were measured at five temperature set points between 10 and 30 °C (typically 10, 15, 20, 25 and 30 °C), which covered the typical night temperature range of the whole growing season. Leaves were acclimated in darkness for at least an hour and then respiration-temperature response was measured in a growth chamber with temperature control (Conviron E15, Winnipeg, Canada). Temperature within the cuvette was controlled to match the ambient temperature in the growth chamber. CO_2 partial pressure in the cuvette was maintained at 400 ppm. At each temperature set point, the leaves were left for 15-20 minutes to stabilize the respiration rate before being recorded. The measurements were made when respiratory gas exchange had equilibrated.

Analysis of photosynthesis and respiration curves

A-C_i curves were analyzed using the biochemical model described by (Farquhar et al. 1980) with parameters from Bernacchi *et al.* (2001) to calculate the parameters potentially limiting photosynthesis: maximum carboxylation rate of Rubisco (V_{cmax}) and RuBP regeneration capacity mediated by maximum electron transport rate (J_{max}). V_{cmax} and J_{max} were adjusted to 20 °C following Leuning (1995), with temperature coefficients from M. H. Turnbull (unpublished data). The photosynthetic rate (A) at saturating light level (2000 µmol CO_2 m^{-2} s^{-1} PPFD) and a C_i of 300 ppm was calculated to compare the photosynthetic capacity between leaves.

The temperature response curves were analyzed using a modified Arrhenius equation described by (Lloyd and Taylor 1994):

$$R = R_0 e^{\frac{E_0}{R_g}\left(\frac{1}{T_0}-\frac{1}{T_a}\right)} \quad (1)$$

where R_0 is the respiration rate at a base temperature T_0 (10 °C, 283 K in our study), T_a is the leaf temperature (K) when R is measured, and R_g is the ideal gas constant (8.314 J mol^{-1} K^{-1}). E_0 is equivalent to the overall energy of activation of the processes, similar but not identical to the energy of activation for a single enzyme reaction, so E_0 should simply be considered a temperature response variable. Previous studies indicated that E_0 appears constant over the physiological temperature range of temperate species (Lyons and Raison 1970). The model was fitted with SigmaPlot 2001 (SPSS Inc., Chicago, IL, USA). Respiration rate at 20 °C was also calculated to compare the respiration rates in moderately high temperature.

The commonly used Q_{10}, which is a simple parameter to measure respiratory temperature response, can be linked to this model by:

$$Q_{10} = e^{\frac{E_0}{Rg}\left(\frac{1}{T_2}-\frac{1}{T_1}\right)} \quad (2) \text{ and,}$$

$$T_1 - T_2 = 10\ (°C) \quad (3)$$

Clearly, as defined by this model, Q_{10} is temperature dependent (Atkin and Tjoelker 2003) and is determined by E_0 at a set temperature. In this study, a Q_{10} of 15 – 25°C was calculated to facilitate comparison with other studies reporting only Q_{10} values.

Leaf analysis

Following the dark respiration measurements, several leaf disks were immediately frozen in liquid nitrogen for protein concentration. Several other leaf disks were homogenized in an extraction buffer and then frozen for Rubisco activity measurements (Tissue *et al.* 1993). The remaining leaf material (excluding the mid-rib and the petiole) was determined for the area using a leaf area meter (Li-3000, Li-Cor Inc. Lincoln NE, USA) and then was dried in a 60 °C oven for a minimum of 48 hrs. The dried leaf material was weighed and ground to fine powder for nitrogen and carbon stable isotope ratio ($\delta^{13}C$) analysis with an Europa 20/20 continuous flow isotope ratio mass spectrometer (CF-IRMS) coupled with an ANCA NT combustion system (Europa, Cheshire, UK) at Lamont-Doherty Earth Observatory. Specific leaf area (SLA) was calculated from the leaf area and dry weight. Leaf nitrogen results were reported on an area (N_{area}) and mass basis (N_{mass}). Leaf protein content was determined on frozen material using the Bradford technique (Sigma-Aldrich, St. Louise, USA). Rubisco activity was measured on homogenized extracts following the protocol reported in Tissue *et al.* (1993).

Tree characteristics

The diameter of each tree was measured at the breast height (1.3m, *D*). Tree and canopy height was determined using an optical hypsometer. The device uses a stationary reflector placed at breast-height and a remote optical device that is alternately pointed at the stationary reflector, and at points of interest. In this case, the top of a top-canopy branch, and the trunk at the lowest canopy branch were used to determine tree height, and height of tree canopy, respectively. Measurements were initially made in July 2003, and duplicated in March 2004 to confirm the match of with- and without-leaf determinations.

Increment cores were taken from each tree, including at least one core taken from the trunk at breast height (~1.3m), to determine both bark thickness, and sapwood radii. The sapwood-heartwood boundary was determined by marking the point of visual translucence when holding the fresh core up to the sunlight. Cores were sealed in straws and kept cool until return to the laboratory. The current sapwood radius, defined as the early-wood portion of the current year, plus the wood portion of the entire previous year was measured (Rodgers and Hinckley 1979, White 1993, Meadows and Hodges 2002). The radii, along with *D*, and bark depth were used to determine the current sapwood areas. Bark depth was measured directly from sapwood cores, but

because coring technique tends to underestimate bark depth, adjustment was made by calculations using allometric equations from Martin (1981).

An additional core was taken from as low on the trunk as possible to correctly age the tree, and to determine the tree's growth rate through time. All cores were dried, mounted and sanded to prepare for age, and growth analysis. Measurement of growth rate was conducted using a Velmex measuring system (Velmex Inc., Bloomfield, NY, USA), a MeasureJ2X® software (VoorTech Consulting, 1998), and a standard microscope. Each core was analyzed twice to minimize error. Age determination was achieved using the cross-dating method, which requires a visual matching of growth ring patterns of all tree-ring sequences and a subsequent dating quality check by the COFECHA program (Holmes 1983). In cases where the center (pith) of the tree was missing, the inside radius of the earliest growth ring was measured, and number of interior rings was estimated by dividing the radius of the missing part by the average annual growth of 10 innermost rings. Accounting for these missing rings, the average number of rings added across trees in all stands was about 4 years. For the majority of cores that missed the pith, the number of estimated missing rings was < 10.

Leaf area index measurement

Stand leaf area index (*L*) and tree-specific leaf area were determined with litter traps and hemispherical photographs. Ten litter traps (70 × 40 cm) that consisted of plastic bins with fine mesh netting inside to keep the leaf litter out of standing water were placed in each stand. Collections of leaf litter were made weekly during leaf fall to minimize decomposition and wind-throw. In this measurement, all leaves collected in 10 traps of one stand were bulked to generate sufficient material for sub-sampling (see below). Fresh leaves were separated by species and their petioles were removed. A sub-sample was scanned (LI-3000, LiCor Inc., Lincoln NE, USA) to determine one-sided surface area. The sorted and separated leaves were then dried in a 70˚ C oven. Each dried sample was weighed to the nearest 0.01 g. A weight to area ratio was determined for each species in each stand using the scanned sub-sample. This ratio was then used to estimate leaf area index (m^2/m^2) in each stand, and the relative contribution of each species (*f*). In mid- to late-summer of 2003, standard methods of hemispherical image capture and analysis were followed to obtain high-resolution digital photos with bracketing exposure to ensure an analyzable image (for a discussion, see Jonckheere *et al.* 2004). The images were analyzed using Gap Light Analyzer (GLA) software (Simon Frazer University, BC, Canada; Institute for Ecosystem Studies, NY, USA) to determine canopy properties including 5-ring (68°) plant area index. A similar procedure was used with the winter images. The value of winter was subtracted from the summer to determine *L* corrected for stem and branch area; subsequently, this result was compared with the litter trap method. The values measured by litter trap and hemispherical photography methods were close, with inter-method differences <0.3.

Canopy carbon exchange model

The one-dimensional, multilayer model NEEMo was used to estimate canopy carbon exchange of stand chronosequence (Whitehead et al. 2004a, Whitehead et al. 2004b). The model incorporates radiative transfer, energy balance, evaporation, photosynthesis and water balance. The canopy was divided into 20 layers based on the vertical distribution of cumulative canopy leaf area index. Total photosynthesis and foliage respiration is calculated separately for sunlit and shaded foliage, and is summed across layers within the canopy to provide daily values. Following Farquhar *et al.* (1980), photosynthesis, A, is calculated as the minimum of the rates limited by the carboxylation, A_c and electron transport, A_q, such that $A = \min(A_c, A_q)-R_d$, where R_d is the rate of daytime respiration resulting from processes other than photorespiration. A_c is dependent on the maximum rate of carboxylation, V_{cmax}, and A_q is dependent on the response of the rate of electron transport, J, to irradiance and its maximum value at saturating irradiance, J_{max} (Farquhar et al. 1980, Farquhar and Wong 1984).Values for the parameters describing the dependence of V_{cmax} and J_{max} on temperature were taken from M. H. Turnbull (unpublished data), using the response described by Leuning (1995). The model incorporates soil water balance and the limiting effects of seasonal root-zone water deficit on canopy photosynthesis. Daily calculations of water balance are used to define a coefficient that estimates the reduction of canopy photosynthesis when daily root-zone water storage falls below 50% of its maximum value. The response of foliage respiration to temperature is described by an Arrhenius function used previously (Turnbull *et al.* 2003). Daily weather data required to drive the model are solar irradiance, minimum and maximum air temperature, and rainfall, with hourly values of weather variables calculated following Goudriaan and van Laar (1994).

Values of the parameters required for the model are listed in *SI Table 4*. Values of V_{cmax}, J_{max}, R_d (assumed to be the same as dark respiration rate R_0), and their seasonal variability were taken from measurements in studied stands during 2003 and from Xu and Griffin (2006). Values of E_0 measured for each stand in June were assumed to be constant throughout the year (Xu and Griffin 2006). The other parameters in the model and the vertical leaf distribution in the canopies were those used at the same site by Whitehead *et al.* (2004b) and assumed to be constant across the stands. Values of L and its seasonality were estimated from hemispherical photography as described by Xu *et al.* (2007).

Estimates of the vertical distribution of photosynthetic and respiration parameters and leaf area were taken from measurements made in one stand and described in more detail in Whitehead *et al*. (2004b).

Long-term survey data

Before 1994, long-term plots were surveyed with a 3 to 10 year interval, so the data do not allow tracking biomass annually. For living trees, biomass were calculated with allometric equations for each survey year, and linearly interpolated for each year during the interval of two surveys. If a tree was an in-growth (reaching D of 2.54 cm) or was

found dead during the interval between two surveys, we allocated the average biomass growth/ loss to all interval years between two surveys.

The 70-year survey data was split into seven 10-year time spans (1937-1946, 1947-1956, 1957-1966, 1967-1976, 1977-1986, 1987-1996, 1997-2006). For stand dominance analysis, growth (or mortality loss) of each tree was calculated for each decade and averaged for 10 years to obtain the mean of annual growth (or mortality loss). The decadal mean of tree AGB was calculated by averaging the biomass of each tree for each year when it was alive. To calculate stand AGB accumulation, aboveground net primary production and mortality loss, tree biomass data were summed for each plot and adjusted relative to the plot area. This method allowed assessing long-term stand dominance and decadal change pattern of AGB.

In this study, we focused on a year-based, rather than stand-age-based, assessment for long-term trend because our data do not allow adjustment of decade-to-decade variation of growth and mortality (*e.g*. caused by climate variability or climate change). The plot effect (stand age difference and site quality) was accounted for with our statistical method (ANCOVA; see Material and methods). The relatively small difference of stand age between these long-term plots (25 years) is not likely to disguise the 70-year long-term trend. Finally, we also conducted a stand-age-based analysis on AGB accumulation, aboveground primary productivity and mortality loss to confirm that the pattern and the results were not essentially different.

Table S1. Plot information

a. Stand chronosequence plots

Plot	Approx. stand age (2003)	Tree density (ha^{-1})	Basal area ($m^2 ha^{-1}$)	Frequency of *Q. rubra* (%)	BA % of *Q. rubra*	Slope (%)	Aspect	Soil pH*	Site index* (1998)
A	35	1581	15.4	36	51	9	E	4.0	55
B	70	754	23.4	35	78	14	NE	4.0	55
C	90	618	27.2	26	51	10	NE	4.0	55
D	135	654	28.8	25	57	6	E	4.0	55

b. Long-term plots (after Schuster *et al.* 2008)

Plot	Stand age (2008)	Basal area 1936 ($m^2 ha^{-1}$)	BA % of *Q. spp.* (1936)	BA % of *Q. rubra* (1936)	Basal area 2006 ($m^2 ha^{-1}$)	BA % of *Q. spp.* (2006)	BA % of *Q. rubra* (2006)	Slope (%)	Aspect	Soil pH	Height in 1998 (mean ± SE)	Site index (1998)
1	123	18.2	29	20	24.6	27	0	11	NW	3.65	24.2 ± 0.7 a	61 (average)
2	123	25.6	31	13	32.1	56	37	9	NW	3.70	24.7 ± 0.8 a	61 (average)
3	123	14.8	96	41	19.6	77	58	11	NW	3.85	18.2 ± 1.0 b	43 (poor)
4	123	13.5	98	6	21.8	80	30	8	NW	4.00	15.8 ± 0.9 b	39 (poor)
5	103	11.4	68	31	28.8	73	73	2	W	4.55	23.8 ± 1.4 ac	61 (average)
6	103	14.5	49	15	36.9	74	58	2	NE	4.25	24.6 ± 0.8 ac	61 (average)
7	108	11.8	99	34	24.7	92	66	11	NE	3.90	20.6 ± 0.4 d	53 (fair)
8	108	10.6	88	43	26.7	86	50	9	NE	3.85	22.2 ± 0.8 cd	57 (fair-average)

*data collected from adjacent plots as an approximate estimation

Table S2. Parameters of tree equations in formula $M=aD^b$ (Brenneman et al., 1978) used in this study to calculate aboveground biomass, with the unit of *D* in inch.

Common name	Scientific name	a	b
Black birch	*Betula lenta* L.	1.6542	2.6606
Black cherry	*Prunus serotina* Ehrh.	1.8082	2.6174
Beech	*Fagus grandifolia* Ehrh.	2.0394	2.5715
Black oak	*Quercus velutina* Lam.	2.4601	2.4572
Chestnut oak	*Quercus prinus* L.	1.5509	2.7276
Eastern hemlock	*Tsuga canadensis* (L.) Carr.	1.3449	2.4500
Pignut hickory	*Carya glabra* (Mill.) Sweet	2.0340	2.6349
Red maple	*Acer rubrum* L.	2.0772	2.5080
Red oak	*Quercus rubra* L.	2.4601	2.4572
Shagbark hickory	*Carya ovata* (Mill.) K. Koch	2.0340	2.6349
Sugar maple	*Acer saccharum* Marsh.	2.4439	2.5735
Scarlet oak	*Quercus conninea* Muench.	2.4601	2.4572
White ash	*Fraxinus americana* L.	2.3632	2.4789
White oak	*Quercus alba* L.	1.5647	2.6887
Yellow birch	*Betula alleghaniensis* Britt.	3.1042	2.3753

Aboveground biomass of some other less common tree species including alder (*Alnus spp.*), black ash (*Fraxinus nigra* Marsh.), black gum (*Nyssa sylvatica* Marsh.), basswood (*Tilia Americana* L.), chestnut (*Castanea dentata* (Marsh.) Borkh.), dogwood (*Cornus florida* L.), grey birch (*Betula populifolia* Marsh.), hop-hornbeam (*Ostrya virginiana* (Mill.) Koch), striped maple (*Acer pensylvanicum* L.), sassafras (*Sassafras albidum* (Nutt.) Nees), shadbush (*Amelanchier canadensis* (L.) Medik.) were calculated with a generic hardwood equation $M=4.5966-(0.2364D)+(0.00411D^2)$ (Monteith 1979), with the unit of *D* in dm. The foliar biomass of red oak was calculated with $M=0.0238D^{1.8600}$ (Hocker and Earley 1983) with the unit of *D* in cm.

Table S3. ANOVA results showing age and seasonal effect on physiological parameters and leaf characteristics. Seasonal effects were integrated as repeated measurements.

Effect	V_{cmax}	J_{max}	A	A_{mass}	PNUE	E_0	$R_{0\,area}$	$R_{0\,mass}$	$R_{0\,N}$	R_{area}	R_{mass}	R_N	A/R	N_{area}	N_{mass}	C/N	$\delta^{13}C$
Age	0.64	0.72	0.49	0.53	0.46	0.70	0.95	0.67	0.48	0.97	0.98	0.66	058	0.48	0.43	0.24	0.56
Season	<0.001	0.02	0.001	<0.001	0.24	0.06	0.02	<0.001	0.01	0.002	<0.001	<0.001	0.05	<0.001	<0.001	<0.001	<0.001
A × S	0.18	0.13	0.19	0.46	0.21	0.78	0.63	0.26	0.39	0.75	0.39	0.57	0.19	0.85	0.84	0.82	0.99

Table S4. Parameters of canopy model

Parameter	Definition	Value	Unit	Reference
L	Leaf area index	See table 3	m^2/m^2	
Ω	Canopy element clumping index	0.84		(Baldocchi and Meyers 1998)
d	Foliage dimension	0.1	m	
V_{cmax}	Maximum rate of carboxylation	This study	µmol m^{-2} s^{-1}	
J_{max}	Apparent maximum rate of electron transport	This study	µmol E m^{-2} s^{-1}	
R_d	Day time respiration other than photorespiration	This study	µmol m^{-2} s^{-1}	
R_0/R_d	Night time respiration to day time respiration ratio	1		
E_0	Energy of activation for respiration as an overall reaction	This study	kJ mol^{-1}	
α	Leaf quantum yield of electron transport	0.22	mol E mol $quanta^{-1}$	(Turnbull *et al.* 2002)
β	Convexity of the light response curve	0.66		(Turnbull *et al.* 2002)
a	Coupling parameter related to intercellular CO_2 concentration	4.0		(Whitehead *et al.* 1996)
g_{s0}	Residual stomatal conductance to CO_2 transfer	0.01	mol m^{-2} s^{-1}	(Whitehead *et al.* 1996)
D_{s0}	Sensitivity of stomatal conductance to air saturation deficit D	1000	Pa	D. T. Tissue and V. Engel (unpublished data)
D_{smin}	Minimum value of D for decreasing g_{s0}	480	Pa	D. T. Tissue and V. Engel (unpublished data)
W_{max}	Maximum root-zone water storage capacity	125	mm	(Whitehead *et al.* 2002). V. Engel (unpublished data)
W_{min}	Maximum root-zone water storage capacity	40	mm	(Whitehead *et al.* 2002). V. Engel (unpublished data)

Figure S1. Forest stand ages within the Highlands Region (based on 451 USFS FIA stands ranging from Connecticut to Pennsylvania, from Schuster 2011)

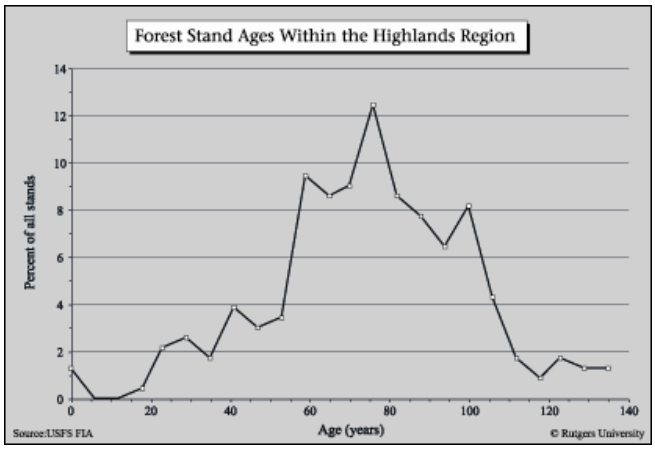

Figure S2. Proportional change for annual canopy carbon fluxes in response to changes in model parameters. Changes in parameters are indicated as ± 40% from the actual values shown as zero change.

Increasing or decreasing V_{cmax} and J_{max} by 40% resulted in less than 20% changes in A_G, but the effect on A_N was more significant (a). Changes in L showed proportional effects on R_f, but less substantial effect on A_G. The adjustment of L in general led to a negative effect on A_N, but the effect was small (< ±7% when L changed between -40% to +20%, c). Increasing or decreasing R_0 up to 40% resulted in proportional effects on R_f, and even greater linear effects (± 60%) on A_N (d). The sensitivity of R_f and A_N to the other respiratory parameter, E_0, showed similar pattern, but carbon fluxes were less affected and the response curve was non-linear (b).

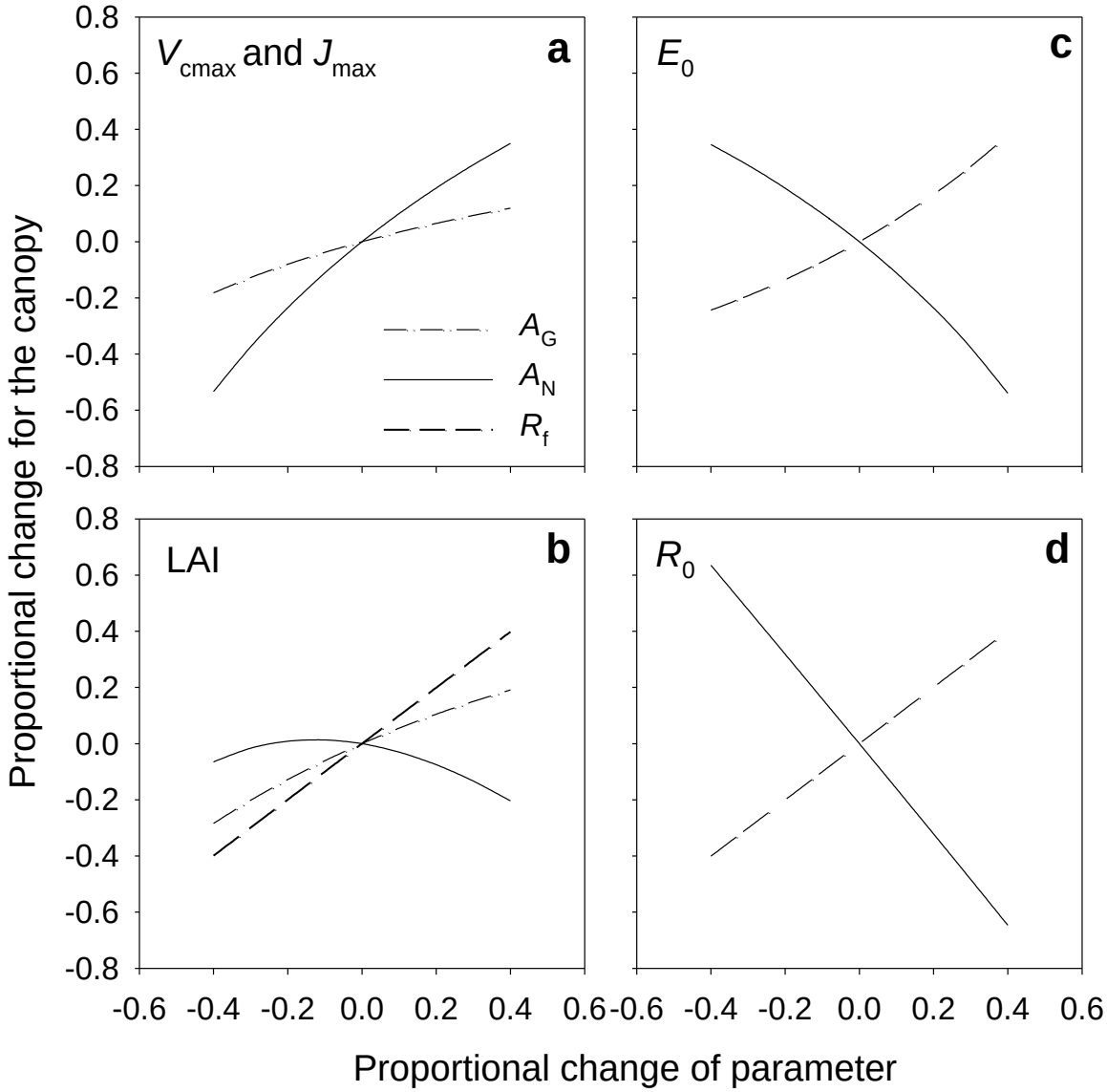

Figure S3. Mortality of individual trees in long-term plots. a) Annual tree deaths, annual mortality, and exponential mortality coefficient in the long-term plots during 1937-2006. Values are shown as mean ± SE. b) Deviation of annual tree deaths, annual mortality, and exponential mortality coefficient among plots (the ratio of standard error to mean).

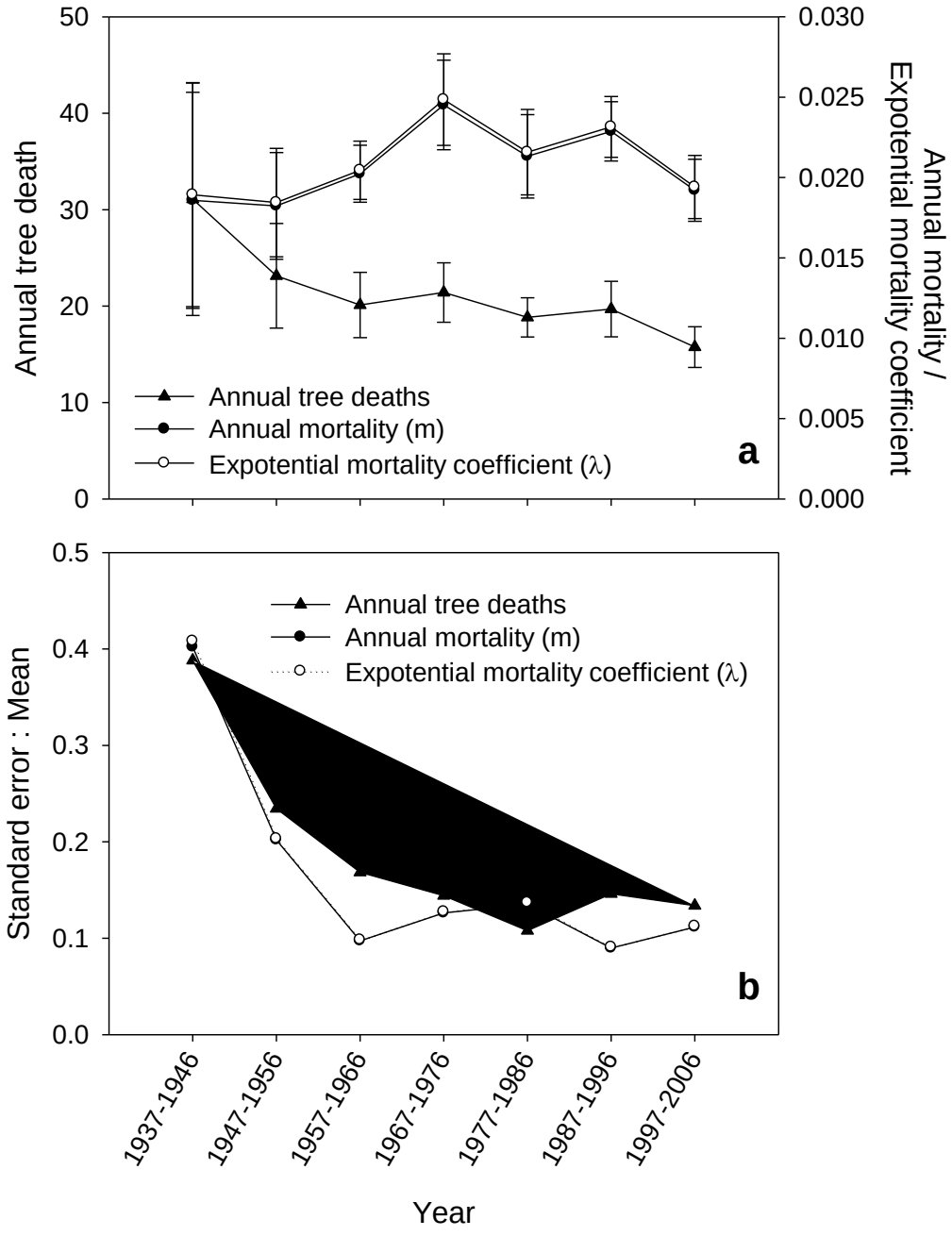

Figure S4. Changes of tree size distribution, the average tree AGB and cumulative AGB over 70 years. a) the change of tree size distribution (histograms) and the average tree AGB (mean ± SE) during 1937-2006. b) the cumulative AGB over tree size (AGB).

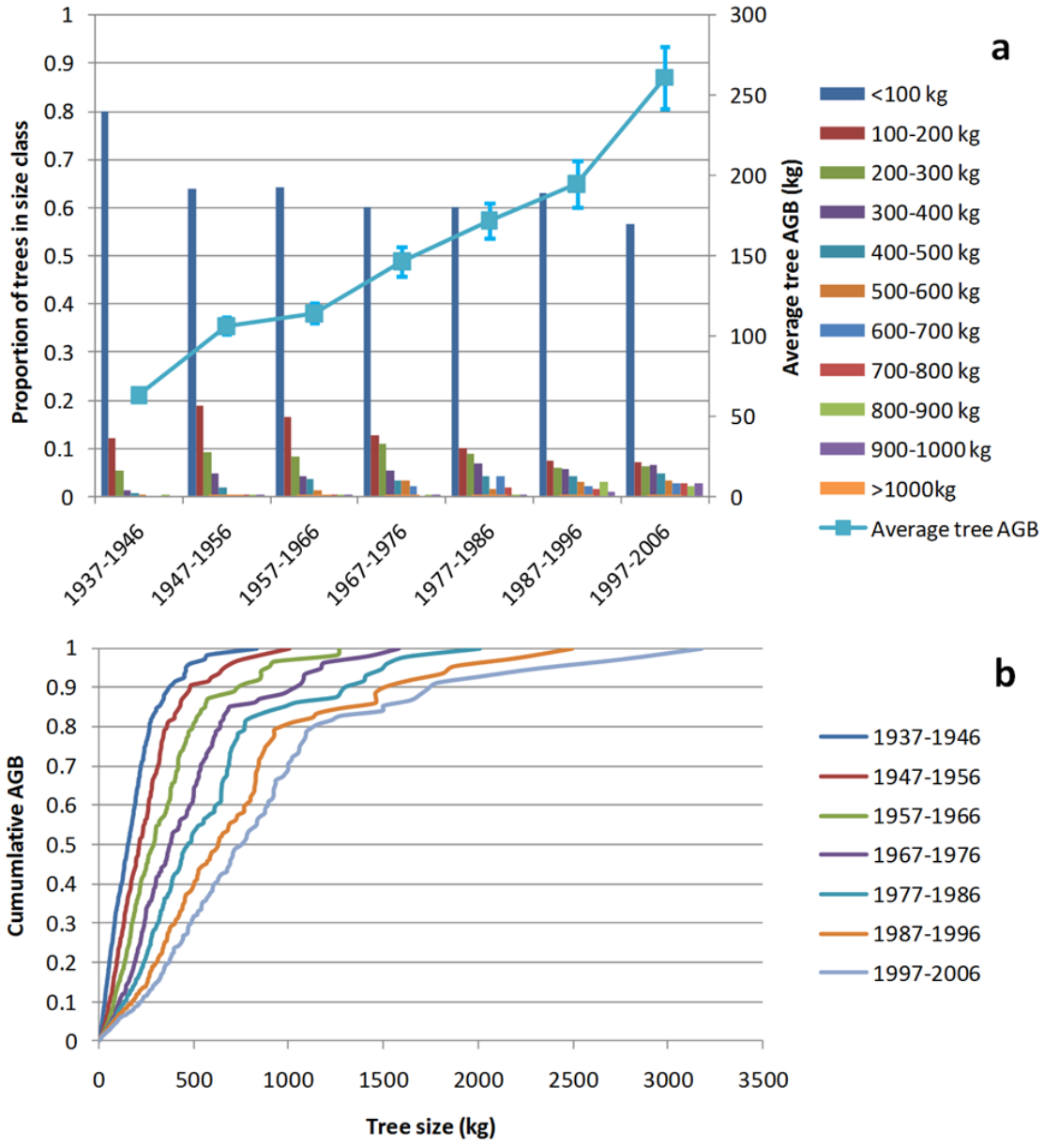

References

Atkin, O. K. and M. G. Tjoelker. 2003. Thermal acclimation and the dynamic response of plant respiration to temperature. Trends in Plant Science **8**:343-351.

Baldocchi, D. and T. Meyers. 1998. On using eco-physiological, micrometeorological and biogeochemical theory to evaluate carbon dioxide, water vapor and trace gas fluxes over vegetation: a perspective. Agricultural and Forest Meteorology **90**:1-25.

Bernacchi, C. J., E. L. Singsaas, C. Pimentel, A. R. Portis, and S. P. Long. 2001. Improved temperature response functions for models of Rubisco-limited photosynthesis. Plant Cell and Environment **24**:253-259.

Farquhar, G. D., S. V. Caemmerer, and J. A. Berry. 1980. A biochemical-model of photosynthetic CO_2 assimilation in leaves of C_3 species. Planta **149**:78-90.

Farquhar, G. D. and S. C. Wong. 1984. An empirical-model of stomatal conductance. Australian Journal of Plant Physiology **11**:191-209.

Goudriaan, J. and H. H. van Laar. 1994. Modelling crop growth processes. Kluwer, Dordrecht, the Netherlands.

Hocker, H. W. and D. J. Earley. 1983. Biomass and leaf area equations for northern forest species. Research report - agricultural experiment station, University of New Hampshire **102**:27.

Holmes, R. L. 1983. Computer-assisted quality control in tree-ring dating and measurement. Tree-Ring Bulletin **43**:69-95.

Jonckheere, I., S. Fleck, K. Nackaerts, B. Muys, P. Coppin, M. Weiss, and F. Baret. 2004. Review of methods for in situ leaf area index determination - Part I. Theories, sensors and hemispherical photography. Agricultural and Forest Meteorology **121**:19-35.

Leuning, R. 1995. A critical-appraisal of a combined stomatal-photosynthesis model for C_3 plants. Plant Cell and Environment **18**:339-355.

Lloyd, J. and J. A. Taylor. 1994. On the temperature-dependence of soil respiration. Functional Ecology **8**:315-323.

Lyons, J. M. and J. K. Raison. 1970. Oxidative activity of mitochondria isolated from plant tissues sensitive and resistant to chilling injury. Plant Physiology **45**:386-&.

Martin, A. J. 1981. Taper and volume equations for selected Appalachian hardwood species. . United States Department of Agriculture Forest Service Research Paper.

Meadows, J. S. and J. D. Hodges. 2002. Sapwood area as an estimator of leaf area and foliar weight in cherrybark oak and green ash. Forest Science **48**:69-76.

Mitchell, K. A., P. V. Bolstad, and J. M. Vose. 1999. Interspecific and environmentally induced variation in foliar dark respiration among eighteen southeastern deciduous tree species. Tree Physiology **19**:861-870.

Monteith, D. B. 1979. Whole-tree weight tables for New York.

Rodgers, R. and T. M. Hinckley. 1979. Foliar weight and area related to current sapwood area in oak. Forest Science **25**:298-303.

Schuster, W. S. F., K. L. Griffin, K. Roth, M. H. Turnbull, D. Whitehead, and D. T. Tissue. 2008. Changes in composition, structure and aboveground biomass over

seventy-six years (1930-2006) in the Black Rock Forest, Hudson Highlands, southeastern New York State. Tree Physiology **28**:537-549.

Schuster, W. S. F. 2011. Chapter 7. Forest ecology. *in* R. E. Lathrop, editor. The Highlands: critical resources, treasured landscapes. Rutgers University Press, New Burnswick, NY.

Tissue, D. T., R. B. Thomas, and B. R. Strain. 1993. Long-term effects of elevated CO2 and nutrients on photosynthesis and rubisco in loblolly pine seedlings. . Plant Cell and Environment **16**:859-865.

Tryon, H. H. 1930. The Black Rock Forest. Cornwall Press, Cornwall, NY.

Tryon, H. H. 1939. Ten-year progress report 1928-1939. Cornwall Press, Cornwall, NY.

Turnbull, M., D. Whitehead, D. Tissue, W. Schuster, K. Brown, V. Engel, and K. Griffin. 2002. Photosynthetic characteristics in canopies of *Quercus rubra*, *Quercus prinus*, *Acer rubrum* differ in response to soil water availability. Oecologia **130**:515-524.

Turnbull, M. H., D. Whitehead, D. T. Tissue, W. S. F. Schuster, K. J. Brown, and K. L. Griffin. 2003. Scaling foliar respiration in two contrasting forest canopies. Functional Ecology **17**:101-114.

White, D. A. 1993. Relationships between foliar number and the cross-sectional areas of sapwood and annual rings in red oak (*Quercus rubra*) crowns. Canadian Journal of Forest Research-Revue Canadienne De Recherche Forestiere **23**:1245-1251.

Whitehead, D., K. L. Griffin, M. H. Turnbull, D. T. Tissue, V. C. Engel, K. J. Brown, W. S. F. Schuster, and A. S. Walcroft. 2004a. Response of total night-time respiration to differences in total daily photosynthesis for leaves in a *Quercus rubra* L. canopy: implications for modelling canopy CO_2 exchange. Global Change Biology **10**:925-938.

Whitehead, D., G. M. J. Hall, A. S. Walcroft, K. J. Brown, J. J. Landsberg, D. T. Tissue, M. H. Turnbull, K. L. Griffin, W. S. F. Schuster, F. E. Carswell, C. M. Trotter, I. L. James, and D. A. Norton. 2002. Analysis of the growth of rimu (*Dacrydium cupressinum*) in South Westland, New Zealand, using process-based simulation models. International Journal of Biometeorology **46**:66-75.

Whitehead, D., N. J. Livingston, F. M. Kelliher, K. P. Hogan, S. Pepin, T. M. McSeveny, and J. N. Byers. 1996. Response of transpiration and photosynthesis to a transient change in illuminated foliage area for a *Pinus radiata* D Don tree. Plant Cell and Environment **19**:949-957.

Whitehead, D., A. S. Walcroft, K. L. Griffin, D. T. Tissue, M. H. Turnbull, V. C. Engel, K. J. Brown, and W. S. F. Schuster. 2004b. Scaling carbon uptake from leaves to canopies: insights from two forest with contrasting properties. Pages 231-254 *in* M. Mencuccini, J. Grace, J. Moncrieff, and K. G. McNaughton, editors. Forests at the land-atmosphere interface. CABI Publishing, Wallingford, UK.

Xu, C. Y. and K. L. Griffin. 2006. Seasonal variation in the temperature response of leaf respiration in *Quercus rubra*: foliage respiration and leaf properties. Functional Ecology **20**:778-789.

Xu, C. Y., K. L. Griffin, and W. S. F. Schuster. 2007. Leaf phenology and seasonal variation of photosynthesis of invasive *Berberis thunbergii* (Japanese barberry) and two

co-occurring native understory shrubs in a northeastern United States deciduous forest. Oecologia **154**:11-21.